C.P. No. 849

C.P. No. 849

MINISTRY OF AVIATION

AERONAUTICAL RESEARCH COUNCIL

CURRENT PAPERS

Low-Speed Tunnel Tests of an Aspect-Ratio 9 Jet-Flap Model, with Ground Simulation by Moving-Belt Rig

by

S. F. J. Butler, B. A. Moy and G. D. Hutchins

LONDON: HER MAJESTY'S STATIONERY OFFICE

1966

EIGHT SHILLINGS NET

U.D.C. No. 533.6.071.1 : 533.682 : 5.001.58 : 533.652.6 : 533.694.6

C.P. No. 849

April 1964

LOW-SPEED TUNNEL TESTS OF AN ASPECT-RATIO 9 JET-FLAP MODEL, WITH GROUND SIMULATION BY MOVING-BELT RIG

by

S. F. J. Butler, B. A. Moy,
and
G. D. Hutchins

SUMMARY

In order to assess the adequacy of the conventional stationary tunnel groundboard technique, particularly for V/STOL models exhibiting large, and often adverse, ground effects, tests have been made on some representative models, including the experiments on a jet-flap model discussed in the present Note. By use of the moving-belt rig, the spurious relative motion between the mainstream and the simulated ground surface could be eliminated and more representative ground boundary-layer flows could be achieved.

With the jet-flap model, the ground boundary-layer condition only had an important influence once jet sheet impingement occurred. Thus, the wing incidence at which an appreciable proportion of the jet efflux flowed upstream along the ground was some 10° higher with the ground surface in motion. The use of a moving ground surface was preferable under these conditions, since it resulted in appreciably higher values of wing lift and stalling incidence, as well as changes in drag, pitching moments and downwash.

Apart from such favourable modifications at very high lift ($C_L \geq 7$), these tests generally confirmed the original fixed groundboard tests, which have been used to predict the take-off and landing behaviour of the B.A.C.126 jet-flap research aircraft.

Replaces R.A.E. Tech Note Aero 2957 - A.R.C. 26078

CONTENTS

		Page
1	INTRODUCTION	4
2	EXPERIMENTAL METHOD	4
	2.1 Moving-belt ground rig	4
	2.2 Model arrangement	5
	2.3 Test procedure	5
	2.3.1 Velocity calibration	5
	2.3.2 Corrections and accuracy	6
	2.4 Strut interference	6
3	AERODYNAMIC INFLUENCE OF THE GROUND BOUNDARY LAYER	7
	3.1 Scope of tests	7
	3.2 Lift and stalling behaviour	8
	3.3 Drag and pitching moments	8
	3.4 Airflow around the wing	9
4	CONCLUSIONS	10
NOTATION		11
REFERENCES		13
TABLE 1 - Model details		14
ILLUSTRATIONS - Figs.1-18		-
DETACHABLE ABSTRACT CARDS		-

ILLUSTRATIONS

	Fig.
Jet-flap model with moving ground	1
Moving ground test arrangement	2
General arrangement of jet-flap model	3
Effect of support strut arrangement on C_L (no tailplane) v. α_w	4(a),(b)
Effect of ground boundary layer on C_L (no tailplane) v. α_w with alternative support strut arrangements	5(a),(b),(c)

ILLUSTRATIONS (Contd.)

	Fig.
Effect of ground boundary layer on C_L (no tailplane) v. α_w	6(a),(b)
Effect of V_G/V_o on C_L (no tailplane) at constant incidence	7(a),(b)
Effect of ground boundary layer on C_T v. C_L^2 (no tailplane)	8(a),(b)
Effect of ground boundary layer on C_m v. C_L (no tailplane)	9(a),(b)
Effect of ground boundary layer on ε v. α_w	10(a),(b)
Flow field with jet impingement on the ground	11(a),(b)
Ground boundary-layer profiles 0.6 local chords behind the wing L.E. plane. Rearward-facing rake	12(a),(b)
Effect of ground surface movement on $\left(\frac{H - p_o}{q_o}\right)_{max}$ in ground boundary layer at 0.6 local chords behind the wing L.E. plane. Rearward-facing rake	13(a),(b)
Ground boundary-layer profiles 3.2 local chords behind the wing L.E. plane. Forward-facing rake	14(a),(b)
Wing upper surface boundary-layer profiles at wing mid-semi-span	15(a),(b)
Chordwise C_p distributions at wing mid-semi-span with $\theta \simeq 50^\circ$, $C_\mu = 0.4$	16(a),(b)
Chordwise C_p distributions at wing mid-semi-span with $\theta \simeq 50^\circ$, $C_\mu = 2.1$	17(a),(b)
Chordwise C_p distributions at wing mid-semi-span with $\theta \simeq 50^\circ$, $C_\mu = 4.0$	18(a),(b)

1 INTRODUCTION

The basic aerodynamic principles[1] for jet-flap wings have now been well established by theoretical and experimental research, partly simulated by the need for basic information and understanding to support the design of the Jet-Flap Research Aircraft by B.A.C. (Luton). In particular, comprehensive balance measurements and flow studies have been made at R.A.E. on a generalised model[2] embodying some of the major design features. These tests included measurements of ground effect, using a conventional, stationary tunnel ground-board. It was found that proximity to the ground produced appreciable changes in downwash at the tailplane as soon as the jet sheet neared the ground, and also caused large reductions in lift and stalling incidence in the presence of jet impingement. Under such conditions, it was considered possible that the unrepresentative boundary-layer on the fixed groundboard could have affected the development of the jet flows over the ground surface, modifying the general air-flow around the model and causing it to differ significantly from the true forward-speed condition.

These particular tests emphasised the general need to assess the reliability of tunnel ground simulation techniques, particularly for V/STOL aircraft configurations exhibiting large, often adverse, ground effects. A natural approach was to eliminate the spurious relative motion between the mainsteam and the ground by substituting a moving surface for the conventional tunnel ground-board, thus ensuring more representative boundary-layer flows on the ground. An elaborate moving-belt rig[3] has therefore been developed at R.A.E., to allow an aerodynamic appraisal of essential ground test techniques for representative models[4].

The present paper describes jet-flap model tests with the moving-belt rig which were made during early 1963.

2 EXPERIMENTAL METHOD

2.1 Moving-belt ground rig

The moving-belt ground rig[3] provides an eight-foot wide belt, capable of speeds up to 90 ft/sec, enclosed within a fairing of overall depth 13 inches spanning the R.A.E. No.2 $11\frac{1}{2}$ ft x $8\frac{1}{2}$ ft wind tunnel (see Fig.1). The rig was designed for use with the tunnel lower balance, models being mounted upside down beneath the moving surface to avoid the necessity for a break in the belt at mid-span (Fig.2). To prevent deformation of the exposed ground surface due to sagging or aerodynamic effects, suction was applied to the inside surface of the belt, constraining it to run flat against a perforated plate. This suction arrangement was also employed to achieve a flat surface during comparative tests with a stationary ground surface.

As the boundary layer on the nose of the fixed fairing was bound to impair the velocity profiles near the moving surface, provision was made for this boundary-layer growth to be removed through a series of slits. Typically[3], in the transverse plane through the model pivot centre, the spatial boundary-layer thickness on the stationary ground belt was about 1.5 inches, with a displacement thickness, δ^*, of 0.27 inches. With the exposed surface moving rearwards at

freestream speed and with suction applied to remove the boundary layer on the nose fairing, δ^* was reduced to about 0.055 inches, and the variation of airspeed near the moving surface was reduced to only 7%.

2.2 Model arrangement

The model closely resembled the one used for the earlier fixed groundboard tests[2]. In particular, the same jet-flap wing was utilised, of aspect ratio 9, with a thick, heavily cambered section (NACA 4424), and a full-span T.E. control, having its unswept hinge-line on the wing lower surface at 89% chord. A high-wing position was again chosen, with $+4^\circ$ dihedral, and the original fin, with a high tailplane position, was also used. However, the fuselage arrangement differed in certain respects. The canopy was omitted, because of the large cutaway which would have been necessary with the modified strut entry arrangement. Further, the fibre-glass fuselage shell was slightly larger than the original wooden fuselage. As previously, transition was fixed on the fuselage nose but not on the wing, the fin or the tailplane.

The model (see Figs.1, 2, 3 and Table 1) was mounted on a vertical, hollow, air-supply strut attached to the moment table of the virtual-centre floor balance, with the usual compressed-air supply connections[5]. Previously, an upright model arrangement had been adopted, but it was necessary to invert the model for the present tests (see section 2.1). Provision was made for distributed suction to alleviate flow separations from the exposed portion of strut, which now entered the model fuselage in the vicinity of the wing root (see also section 2.4).

Pitching moments have been referred to the model pivot centre, in the transverse plane through the wing mean quarter-chord point but displaced vertically relative to it (see Fig.3). At the chosen wing mean-quarter-chord clearance from the ground, $1.5\bar{c}$, the wing incidence was restricted to 20°, at which incidence the tail of the fuselage touched the ground.

2.3 Test procedure

2.3.1 Velocity calibration

The distribution of the mainstream air flow between the upper and the lower sections of the divided tunnel was determined as before[2]. Thus, with the various model configurations, the mean speed (V_o) in the test section was determined by measurements of the mean speed ahead of the ground (V_A) and above it (V_U). The injection of high momentum air was again found to induce a larger proportion of the tunnel mainstream air to pass through the test section. Thus, in the extreme case of $C_\mu = 4.0$, the increase in the ratio (V_o/V_A) amounted to 2.5%. Under conditions of jet impingement, however, such jet induction effects were counterbalanced by jet blockage effects, to a greater or lesser extent (see Ref.2).

The main tests were made using suitable values of V_A to achieve the desired value of V_o for a specific model configuration. Particular care was

taken to ensure that the same test speed was used for comparative tests with and without a moving ground surface. To this end, further speed checks were provided by three pitot-statics ahead of the model at the start of the test section (see Ref.3).

2.3.2 Corrections and accuracy

Tunnel lift constraint corrections were not applied, because the estimated effect of the other three boundaries was extremely small.

Allowance was made for model and strut guard solid blockage, and for wake blockage, based on the plain-wing C_{D_o}. However, no further wing wake blockage corrections were applied, due to the absence of a method suitable for the mixed flow occurring when the wing jet passes close to or impinges on the ground. Thus, the test speed, on which all coefficients (including C_μ) were based, was less accurately known under the conditions of the ground effect tests. The trends should be correctly indicated, but the precise values of the force and moment coefficients may be somewhat inaccurate near maximum lift.

The main reservation concerns the possible effect of strut interference, as discussed in the following section. However, although the absolute accuracy was certainly reduced on this account, much smaller effects would be expected on the changes resulting from belt motion.

2.4 Strut interference

It was appreciated that the necessity for a strut entry into the fuselage upper surface was particularly unfortunate with a high-wing position for the jet-flap wing. Earlier tests[2] had shown that as much as 15% of the total lift arose from pressures on the fuselage. Moreover, the wing usually stalled as the result of the spread of inboard separations commencing ahead of the blowing slot near the wing root, i.e. in close proximity to an upper strut entry. Some aerodynamic interference effects from the presence of the strut were expected, even if strut-induced separations were suppressed. To alleviate flow separations from the exposed strut, a B.L.C. arrangement was provided, with distributed suction through a perforated surface. However, preliminary tuft studies showed that mere suppression of strut flow separations was not sufficient to eliminate the associated flow separations from the nearby fuselage surface. With a lower strut, the upper fuselage flow had been well-attached, with pronounced induced flows in the vicinity of the flap root at the higher C_μ-values. However, there was now a tendency for separations behind and to either side of the strut, which increased in severity at high C_L-values. The measured lift coefficients were appreciably smaller than those measured in the comparable tests with a lower strut entry, and the wing stalling behaviour at high C_μ-values was noticeably affected (see Fig.4).

Consequently, additional control was provided on the fuselage by blowing through a set of 3 flattened tubes* attached to the strut guard, with one nozzle

---

* Each tube had a rectangular exit of width 0.4 inches and depth 0.07 inches.

at the rear and the other two on either side of the support strut. These nozzles were so arranged that their efflux spread over the fuselage surface; the total blowing rate was equivalent to a C_μ of about 0.013 (for main wing C_μ-values up to 2.1) or 0.025 ($C_\mu = 4$). As the tubes were attached to the strut guard, rather than to the model, their effectiveness depended on the incidence range which was required. Two arrangements were tried, providing wing incidence ranges of 0° to 20° and 10° to 20° respectively. With the latter arrangement, the general agreement with the earlier lower-strut tests[2] was good (see Fig.4), although the lift was still some 5% less. With the alternative arrangement allowing a full incidence range, the agreement was appreciably poorer, but tuft studies showed that the wing stalling behaviour nevertheless was closely similar to that observed in the original tests. For convenience, this arrangement was later used for the main set of tests described in section 3 (Fig.6 onwards).

Prior to these main tests, some preliminary comparative tests were made with and without a moving ground surface, with the two alternative fuselage B.L.C. arrangements as well as without fuselage B.L.C. With each of the three strut entry arrangements, higher C_L-values were measured with improved ground simulation ($V_G = V_o$) once jet impingement occurred (see Fig.5). Although the actual magnitude of the lift increments showed some dependence on the strut entry conditions, the general conclusions regarding the effect of ground motion were not affected.

3 AERODYNAMIC INFLUENCE OF THE GROUND BOUNDARY-LAYER

3.1 Scope of tests

Following the investigation of strut interference effects* already discussed (see section 2.4), a strut entry arrangement was selected for the main tests which allowed a full wing incidence range of 20°. Throughout the tests, a wing mean-quarter-chord clearance from the ground of $1.5\bar{c}$ was used, which corresponded to a practical touchdown condition, and coincided with the smallest clearance considered in the original fixed groundboard experiments. Generally, comparative tests were made to establish the difference in behaviour with the ground belt stationary (representative of a conventional, fixed groundboard) and with the exposed surface of the ground belt moving rearwards at the mainstream speed to ensure more representative ground boundary-layer development. A few additional tests were made with systematic variation of the ratio of ground surface speed to mainstream speed.

Usually, a full-span T.E. control angle of 30° was employed, corresponding to a mean jet deflection angle, θ, of about 50° relative to wing chord, with a range of C_μ-values from 0 to 4; some tests were also made at $C_\mu = 2.1$ and 4 with the T.E. control angle 0° ($\theta \simeq 20°$). For each configuration, measurements were first made of lift, drag and pitching moments without the tailplane, and then with different tailplane settings to derive mean downwash.

---

* Because of such effects, the present results should not be compared directly with the earlier, fixed groundboard tests.

The nature of the interaction between the ground boundary layer and the impinging jet sheet was investigated with $\theta \simeq 50^{\circ}$ and $C_{\mu} = 0.4$, 2.1 and 4.0. Some typical wing surface pressure distributions were measured and boundary-layer profiles were obtained on both the wing and the ground surface. Also, the general airflow around the wing was studied, including the stalling behaviour, using surface tufts and a tuft grid.

The usual test speed of 80 ft/sec corresponded to a wing Reynolds Number of 0.37×10^{6} (based on aerodynamic mean chord); to achieve $C_{\mu} = 4.0$, the test speed was reduced to 60 ft/sec.

3.2 Lift and stalling behaviour

The effect of the ground boundary-layer condition on lift is shown in Fig.6. In the absence of jet impingement, there were only small differences between the lift curves with the ground belt stationary and moving at freestream speed. Under conditions of jet impingement, which occurred with $\theta = 50^{\circ}$ for incidences exceeding 15°, 5° and 0° at $C_{\mu} = 1.3$, 2.1 and 4.0 respectively, improved ground simulation ($V_G = V_o$) resulted in increased lift.

Some tests with a range of values for the ratio, V_G/V_o, of ground belt speed to freestream speed, showed a gradual variation of lift, suggesting a progressive change in airflow pattern as the ground boundary-layer condition was varied (see Fig.7).

Improved ground simulation also resulted in increases in stalling incidence when there was jet impingement (Fig.6). However, the character of the wing stall near the ground was much the same as with a stationary ground, with a tendency for leading-edge separations to occur at the higher C_{μ}-values. This behaviour was not encountered outside ground effect, where the wing invariably stalled[2] (at appreciably higher incidences) as the result of the spread of flow separations starting just ahead of the T.E. flap near the wing root.

3.3 Drag and pitching moments

The ground boundary-layer condition only affected drag materially in the presence of jet impingement, when improved ground simulation (i.e. $V_G = V_o$) resulted in a significant reduction in drag at constant lift (see Fig.8). The corresponding pitching-moment curves, without the tailplane, also were somewhat straighter with the ground surface moving (see Fig.9).

The original stationary groundboard tests[2] showed large reductions in the mean downwash at the tailplane as soon as the jet sheet neared the ground. Although similar trends were found in the present tests, the quantitative agreement of the stationary groundboard tests was poor (see Fig.10), even without jet impingement. Presumably, this difference was at least partly due to increased strut and strut guard interference with the revised strut entry arrangement. Evidence of such interference was provided by tailplane power reductions which were encountered at the higher incidences in the present tests. Consequently, it was necessary to consider the present results strictly on a comparative basis.

At C_μ = 0.4, representative of the results obtained without jet impingement, the effect of the ground boundary layer on downwash was not significant (see Fig.10). With jet impingement, illustrated by the curves for C_μ = 2.1*, there was some increase in downwash with the ground belt moving. However, even if the original fixed groundboard results were modified to incorporate changes of this magnitude, the major reductions in downwash due to ground effect would still remain.

3.4 Airflow around the wing

Apart from minor changes in mean downwash at the tailplane, it was clear that variation of the ground surface boundary condition only caused significant differences in model behaviour in the presence of jet impingement. A detailed study was therefore made of the nature of the interaction between the impinging jet and the local surface flows on the ground. The general airflow pattern was investigated, using a grid of tufts located at mid-semi-span of the wing, with surface tufts on the wing and on the stationary ground. Further, some boundary-layer profiles were measured on the ground surface upstream and downstream of the impinging jet, and on the upper surface of the wing. Typical wing surface pressure distributions were also obtained.

The tuft grid showed that improved ground simulation (with $V_G = V_o$) appreciably delayed the incidence at which a substantial proportion of the impinging jet flowed upstream along the ground (Fig.11). This was confirmed by the boundary-layer traverse on the ground ahead of the impingement region, with a rearward-facing rake (see Fig.12). The jet flow readily penetrated the low-head boundary-layer region close to the stationary ground surface. However, with the ground surface moving rearwards, a more uniform jet penetration** occurred at incidences some 10° higher at both C_μ = 2.1 and C_μ = 4.0 (see Fig.13). Motion of the ground surface did not lead, however, to any pronounced changes in the behaviour of the rearward component of the impinging jet (see Fig.14).

Whether the ground surface was moving or stationary, the forward-flowing part of the jet separated to form a vortex-type flow between the wing and the ground, with outward flow towards the wing tip (see Fig.11 and Ref.2). However, with the ground surface moving, the reduced jet penetration led to a reduction in the size of the associated vortex and permitted the increased wing circulation indicated by the lift measurements already described.

---

* Although comparative downwash measurements were attempted at C_μ = 4.0, the results showed considerable scatter and did not merit inclusion.

** The sensitivity of the forward flowing jet to ground boundary condition indicated that the magnitude of the measured ground effect probably depended on the jet velocity ratio as well as the more usual correlation parameter of the momentum coefficient. Thus, at a prescribed value for C_μ, it could be argued that greater forward penetration and larger adverse ground effects, might be expected to accompany an increase in jet velocity (by reduction of slot width), and vice versa.

The wing lift changes were reflected in the observed wing surface pressure distributions. Thus, in the absence of impingement, the ground boundary condition scarcely affected the pressure distributions (Fig.16). However, in the presence of impingement, improved ground simulation ($V_G = V_o$) not only increased the negative pressures on the wing upper surface but also reduced the negative pressure region on the wing lower surface associated with the strength of the vortex flow between the wing and the ground (Figs.17, 18). The increased wing circulation with the belt moving would be expected to be accompanied by a rearward shift of the nose stagnation point around the wing lower surface, which in fact occurred.

At the chosen spanwise position, no striking differences were apparent between the upper surface boundary-layer profiles at 40% chord $V_G = 0$ and for $V_G = V_o$ (see Fig.15). This was perhaps surprising, in view of the pronounced effect of movement of the ground surface on stalling behaviour (see section 3.2). Much more detailed investigations nearer the wing nose would have been necessary to obtain a better understanding of the tendency towards L.E. separations, which has only been detected inside ground effect on the present model. However, some guidance may be obtained from turbulent boundary-layer calculations, by the method of Ref.6, which suggest that critical conditions for the occurrence of turbulent separation would be expected to be attained simultaneously over an appreciable extent of the chord with the observed velocity distributions.

4 CONCLUSIONS

Following earlier tests with a conventional stationary tunnel groundboard, some experiments have now been made on a jet-flap model, using the R.A.E. moving-belt rig for ground simulation. Because of the necessity to avoid a break in the moving surface, the model was supported by a strut entering the upper side of the fuselage. Consequently, some difficulties were encountered due to strut interference and fuselage flow separations, necessitating the provision of auxiliary B.L.C. devices in the vicinity of the strut entry.

Comparative tests were made to establish the difference in model behaviour with the usual stationary ground surface, and with the ground surface moving downstream at freestream speed to ensure improved simulation. Provided that the wing jet efflux did not actually impinge on the ground surface, no material differences were found, except for some minor downwash changes at the tailplane position. Once jet impingement occurred, however, the general airflow around the wing was affected, particularly the interaction between the jet sheet and the ground surface. With the ground surface moving downstream at freestream speed, rather than stationary, the incidence at which an appreciable proportion of the jet efflux flowed forwards was delayed by some 10°, allowing increased circulation around the wing.

Such flow changes, with the moving surface to improve ground simulation, resulted in appreciably higher values of lift and stalling incidence, as well as drag reductions and changes in pitching moments and downwash. For example, at $C_\mu = 4$, $\theta \simeq 50^\circ$, the maximum lift coefficient was increased by about 10%.

The general reliability of the original fixed groundboard tests, which have been used to predict the behaviour of the B.A.C. 126 jet-flap research aircraft inside ground effect, has been confirmed, apart from the need for some favourable modifications at very high lift ($C_L \geq 7$).

NOTATION

A_t blowing slot area

b wing span

$c, \bar{c}, \bar{\bar{c}}$ wing chord, (local, standard mean, and aerodynamic mean)

C_D, C_T drag and thrust coefficients $= \frac{D}{q_o S}, \frac{T}{q_o S}$

C_L lift coefficient $= \frac{L}{q_o S}$

C_m pitching moment coefficient $= \frac{m}{q_o \bar{\bar{c}} S}$

C_p surface pressure coefficient

C_μ momentum coefficient $\frac{M_j V_j}{q_o S}$

h mean wing clearance from ground surface

H total head in boundary layer

$\frac{H - p_o}{q_o}$ boundary layer coefficient

ℓ_t tail arm

M_J mass-flow rate

p_o mainstream static pressure

q_o mainstream dynamic head, based on V_o

NOTATION (Contd.)

S	gross wing area
S'	reference wing area corresponding to spanwise extent of jet slot
S_t	tailplane area
S_F	fin area
V_A	mean speed ahead of ground
V_G	mean speed of ground surface
V_o	mainstream speed (below ground for present tests)
V_J	jet speed
V_U	mean speed above ground
x/c	chordwise position of present-plotting orifice
y	distance from surface for boundary-layer traverses
α_w	wing incidence (degrees)
δ^*	boundary-layer displacement thickness
ε	mean downwash at tailplane (degrees)
θ	effective jet deflection angle (degrees)

REFERENCES

No.	Author	Title, etc.
1	Williams, J. Butler, S.F.J. Wood, M.N.	The aerodynamics of jet-flaps. A.R.C. R & M 3304, January 1961
2	Butler, S.F.J. Guyett, M.B. Moy, B.A.	Six-component low-speed tunnel tests of jet-flap complete models with variation of aspect ratio, dihedral, and sweepback, including the influence of ground proximity. A.R.C. R & M 3441, June 1961
3	Butler, S.F.J. Moy, B.A. Pound, T.N.	A moving-belt rig for ground simulation in low-speed wind tunnels. A.R.C. R & M 3451, December 1963
4	Williams, J. Butler, S.F.J.	Further developments in low-speed wind-tunnel techniques for V/STOL and high-lift model testing. A.R.C. 25849, January 1964
5	Butler, S.F.J. Williams, J.	Further comments on high-lift testing in wind tunnels, with particular reference to jet-blowing models. Aero Quarterly Vol XI, pp 285-308, August 1960
6	Head, M.R.	Entrainment in the turbulent boundary layer. A.R.C. R & M 3152, September 1958

TABLE 1

Model data

S	604.5 sq in.
b	74.50 in.
c_{root}	11.00 in.
c_{tip}	5.33 in.
$\bar{c}$	8.09 in.
$\bar{\bar{c}}$	8.46 in.
Aspect ratio	9.20
Taper ratio	0.485
Wing/body angle	5°
Quarter-chord sweepback	6°
Hinge-line sweepback	0°
Dihedral	4°
Model centre position	0.25 $\bar{\bar{c}}$ (see Fig.3)
ℓ_t	36.0 in.
S_t	122.3 sq in.
S_F	106 sq in.
Blown wing area S'	503 sq in.
A_t	2.91 sq in.
Inboard limit of nozzle	0.116 b/2
Outboard limit of nozzle	0.972 b/2
Inboard width of nozzle	0.060 in.
Outboard width of nozzle	0.031 in.

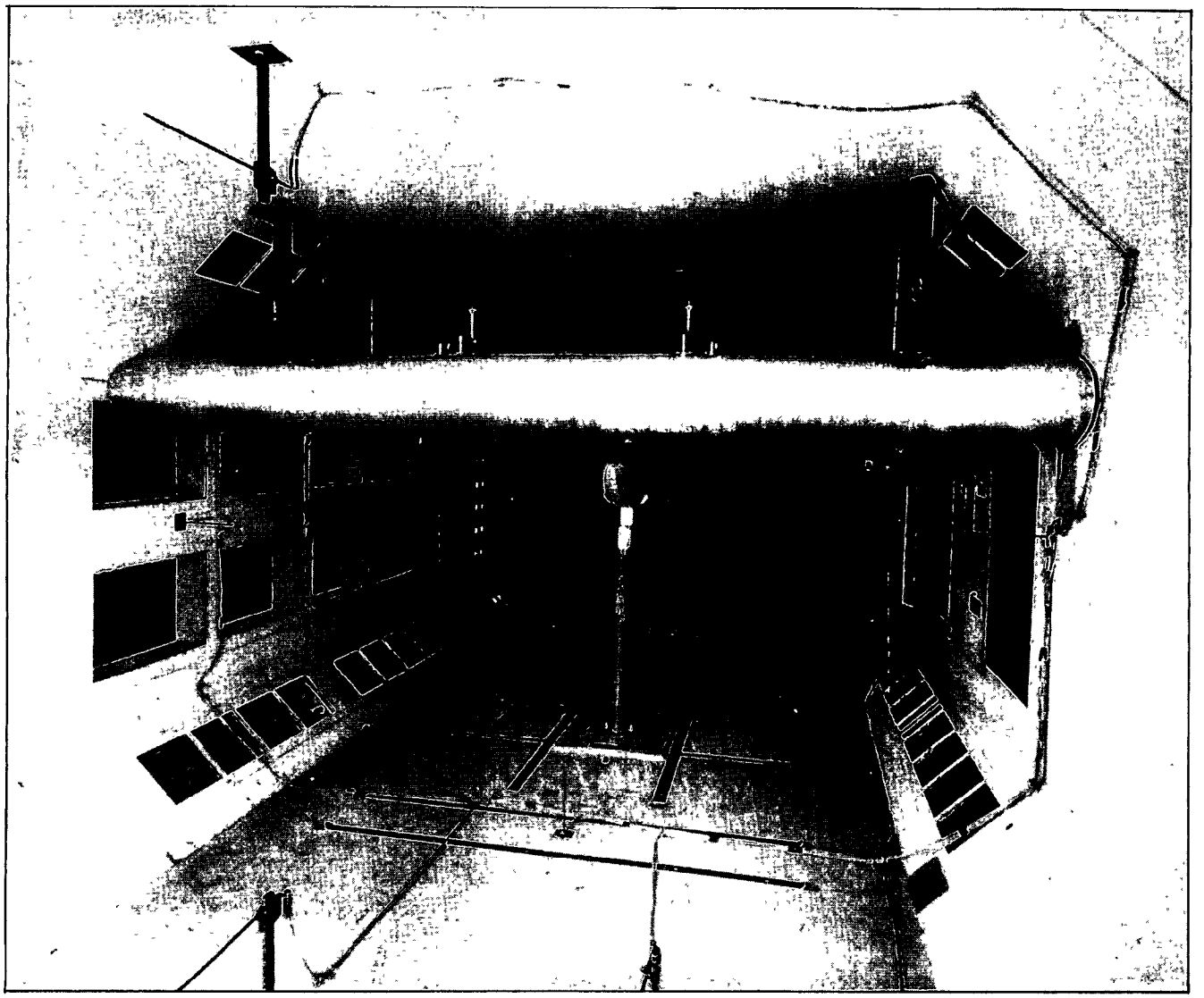

FIG.1. JET - FLAP MODEL WITH MOVING GROUND

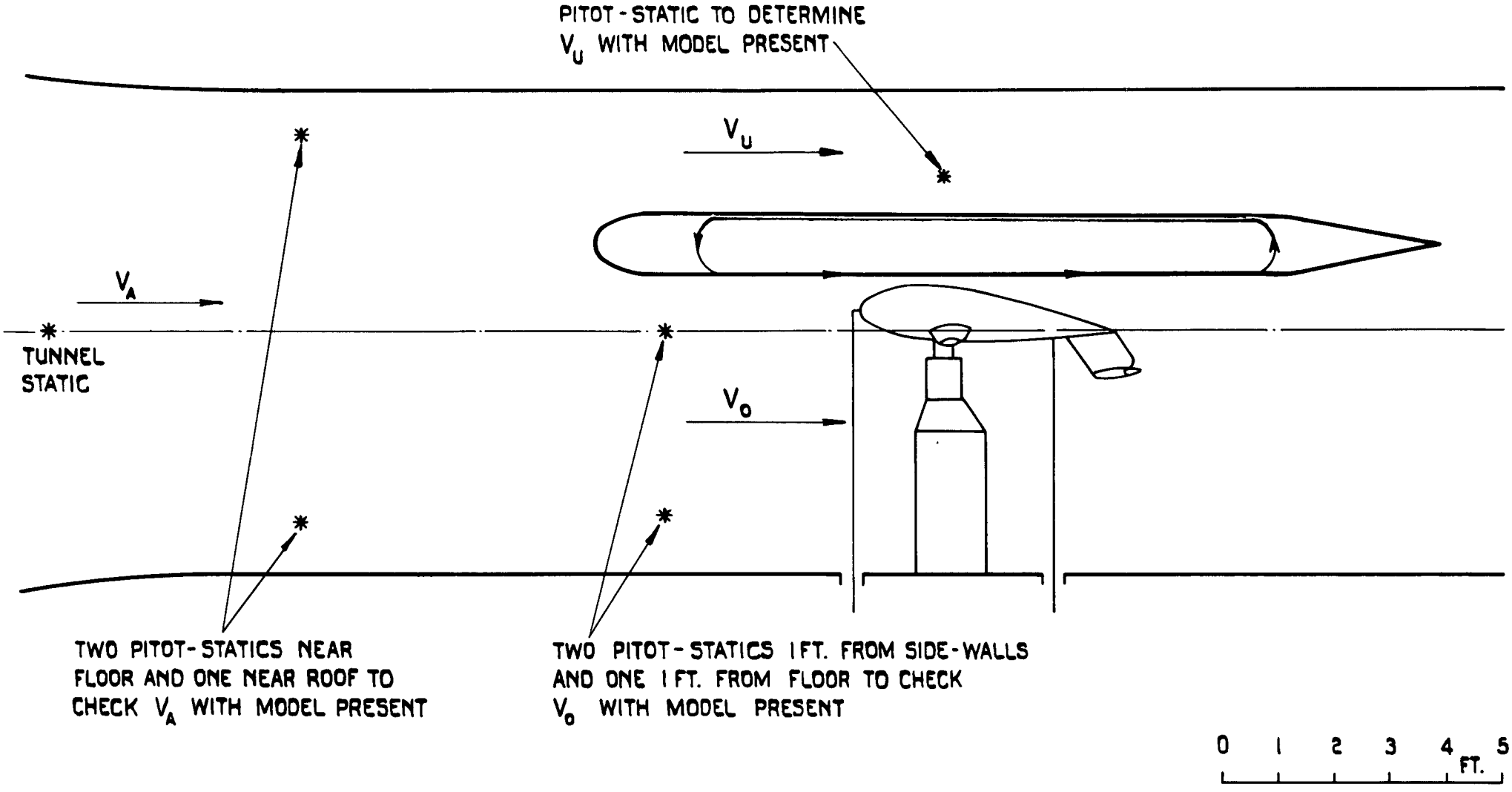

FIG. 2. MOVING GROUND TEST ARRANGEMENT.

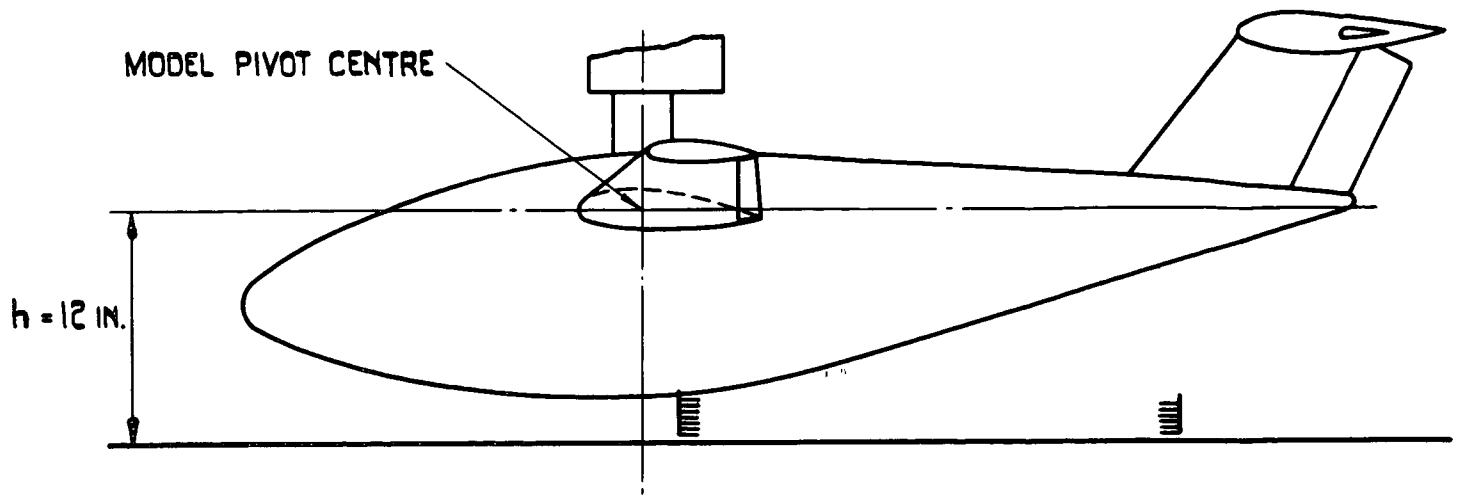

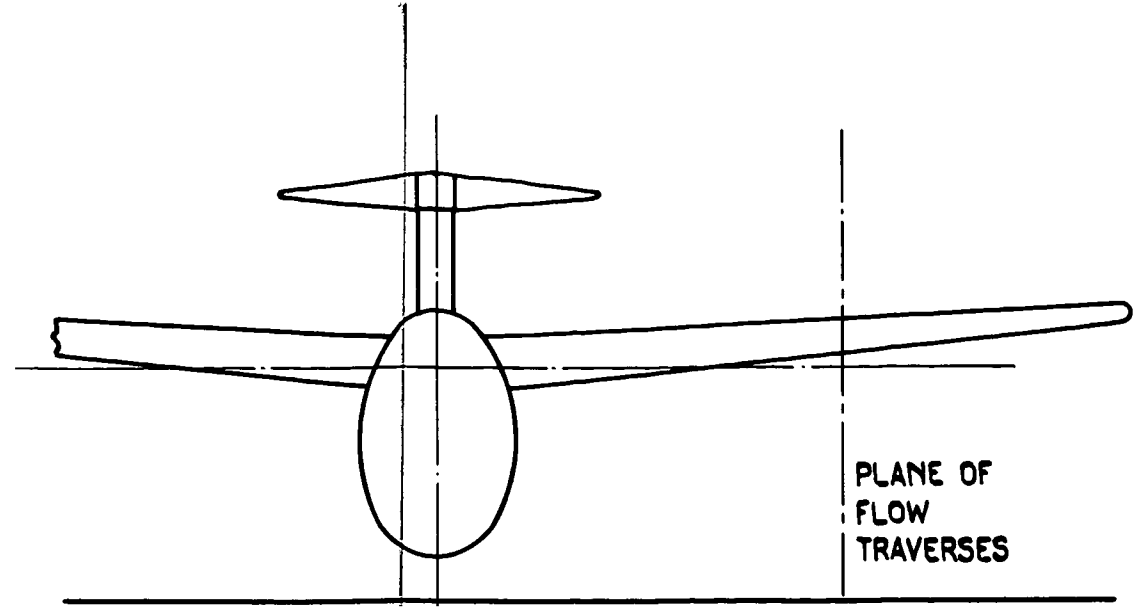

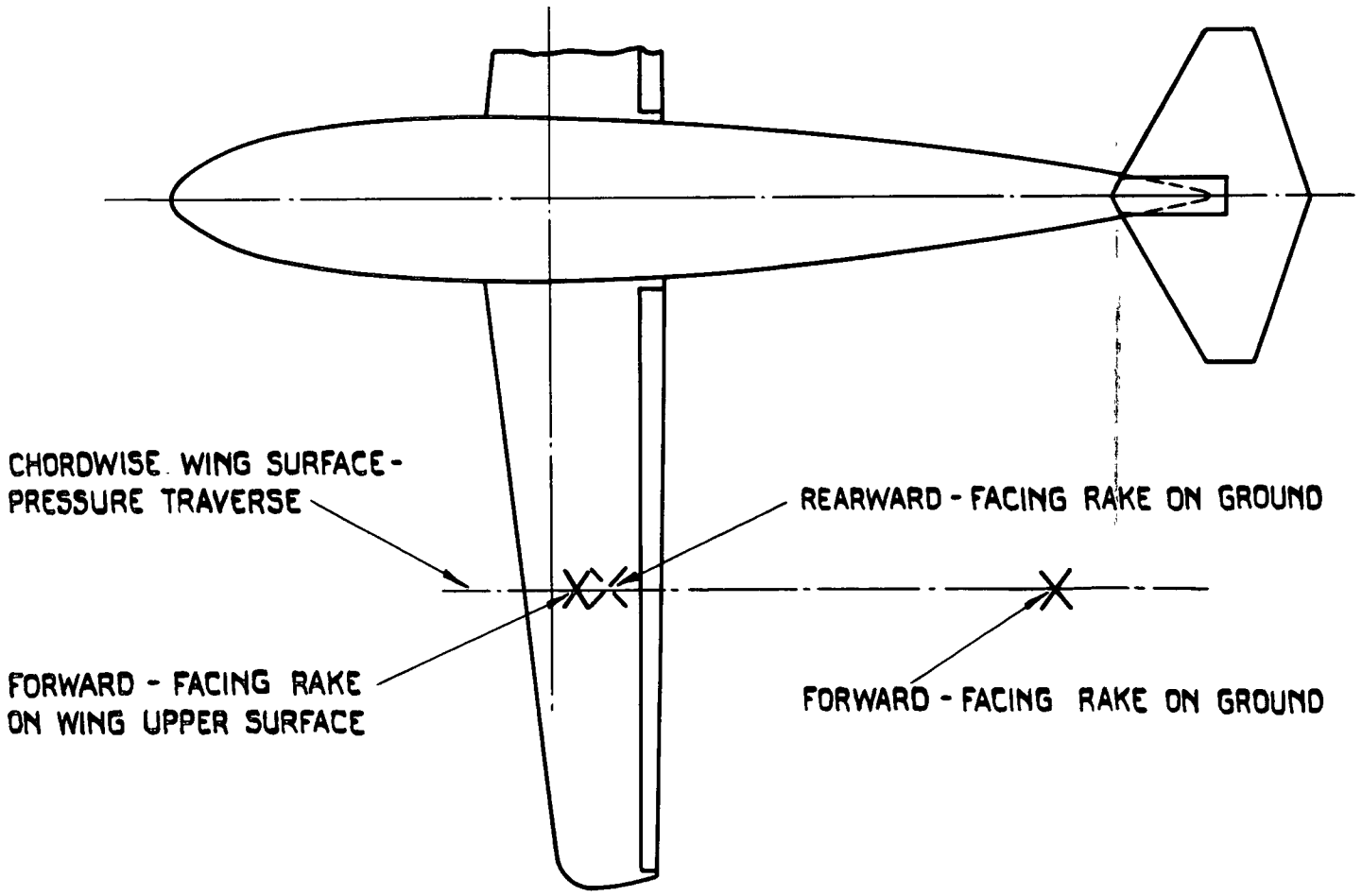

PRINCIPAL MODEL DETAILS.

S	604·5	SQ.IN.	T.R.	0·485
b	74·5	IN.	WING/BODY ANGLE	5°
C_{ROOT}	11·0	IN.	QUARTER-CHORD SWEEP	6°
C_{TIP}	5·33	IN.	HINGE-LINE SWEEP	0°
$\bar{C}$	8·09	IN.	DIHEDRAL	+ 4°
$\bar{\bar{C}}$	8·46	IN.	S_t	122·3 SQ. IN.
AR	9·20		ℓ_t	36·0 IN.

MODEL SCALE

0 10 20 IN.

FIG. 3. GENERAL ARRANGEMENT OF JET-FLAP MODEL

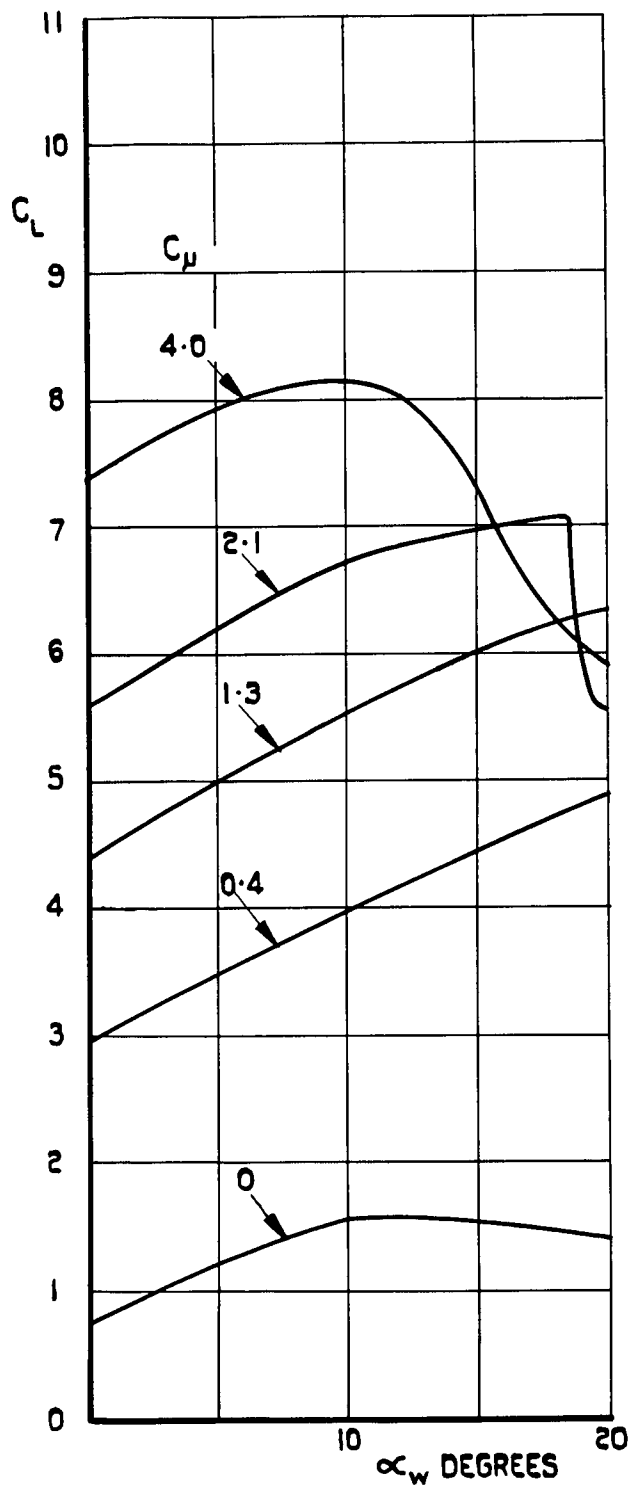

(a) LOWER STRUT.

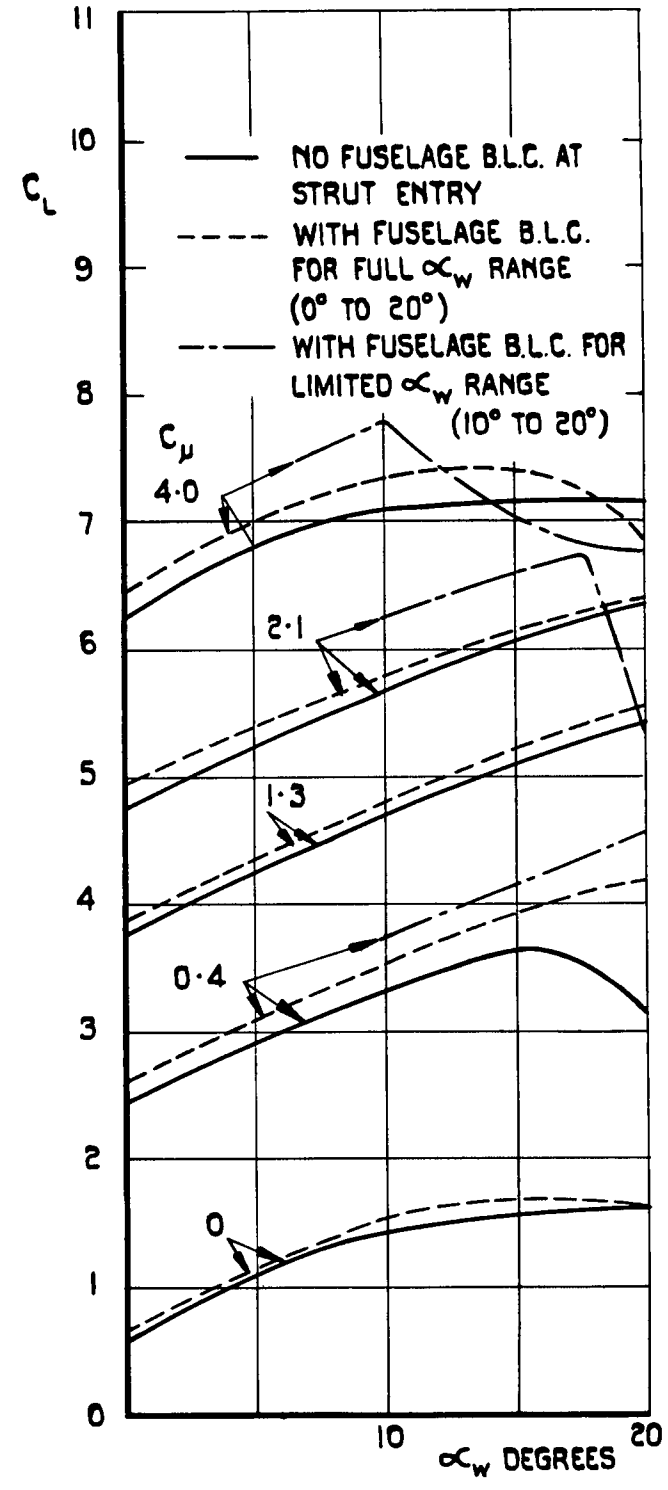

(b) UPPER STRUT, WITH SUCTION B.L.C. ON EXPOSED STRUT.

FIG. 4. EFFECT OF SUPPORT STRUT ARRANGEMENT ON C_L (NO TAILPLANE) v α_w.
CONTROL ANGLE = 30° ($\theta \triangleq 50°$), GROUND CLEARANCE 1·5 $\bar{c}$,
GROUND SURFACE STATIONARY.

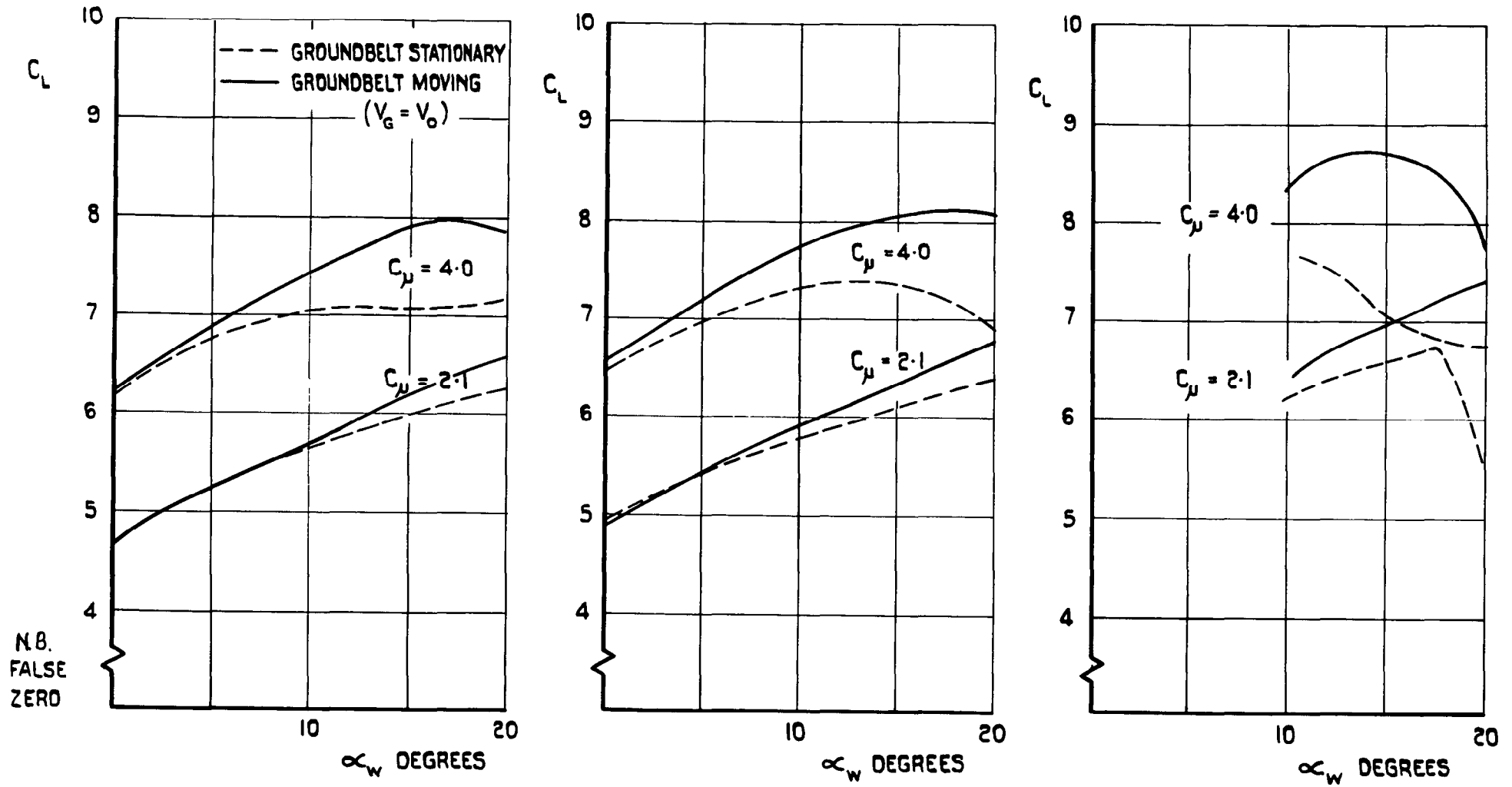

(a) NO FUSELAGE B.L.C. AT STRUT ENTRY.

(b) WITH FUSELAGE B.L.C. FOR FULL α_w RANGE (0° TO 20°).

(c) WITH FUSELAGE B.L.C. FOR LIMITED α_w RANGE (10° TO 20°).

FIG.5. EFFECT OF GROUND BOUNDARY LAYER ON C_L (NO TAILPLANE) $v\alpha_w$ WITH ALTERNATIVE SUPPORT STRUT ARRANGEMENTS. CONTROL ANGLE = 30°($\theta \doteq 50°$), GROUND CLEARANCE 1·5$\bar{\bar{c}}$, GROUND SURFACE STATIONARY.

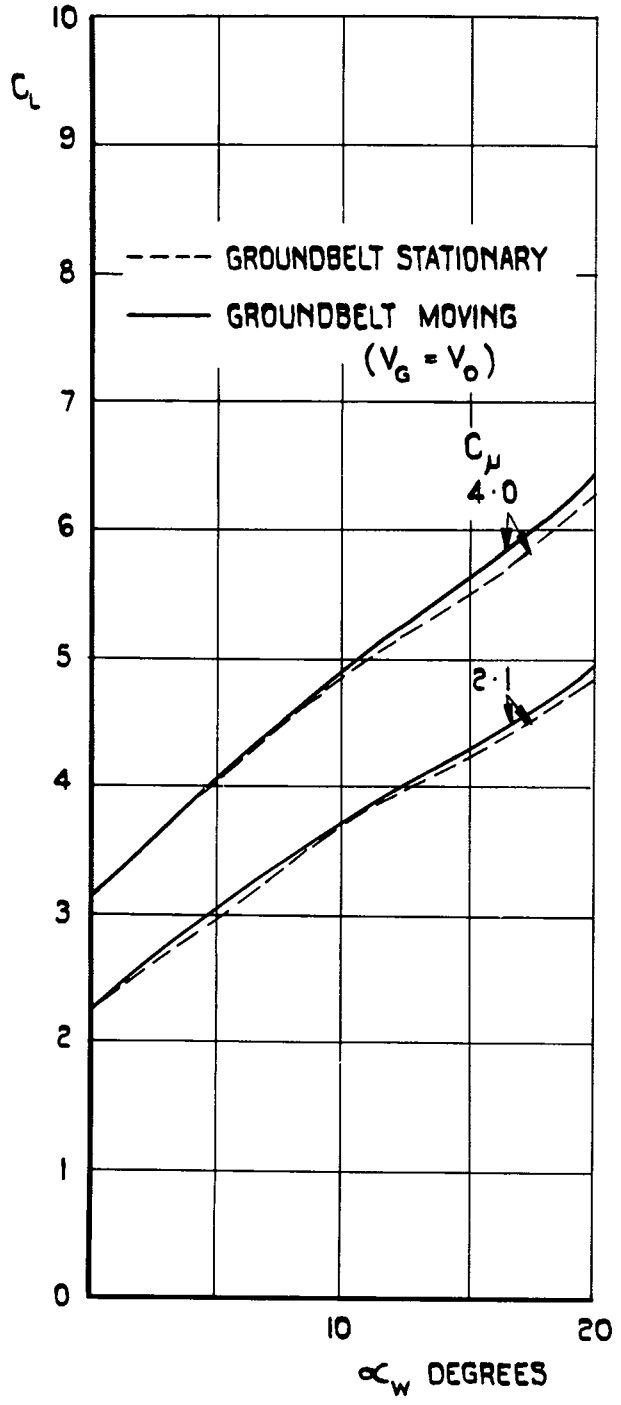

(a) CONTROL ANGLE = 0°
($\theta \triangleq 20°$).

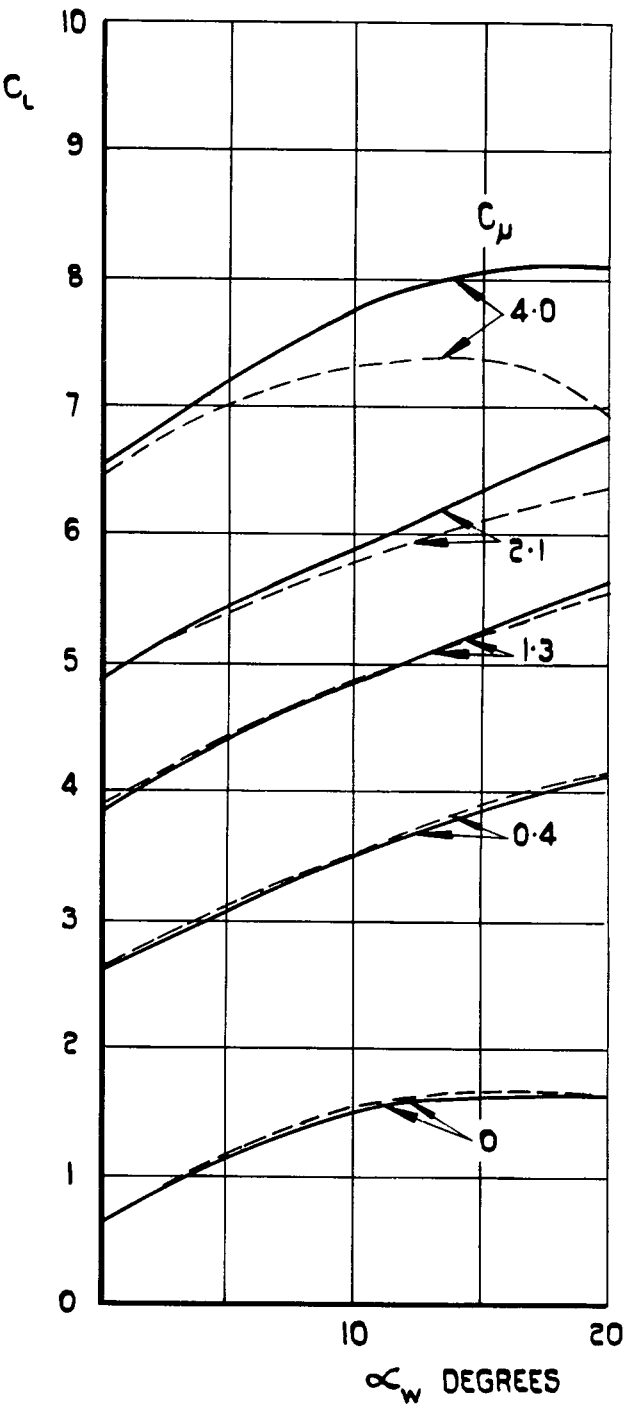

(b) CONTROL ANGLE = 30°
($\theta \triangleq 50°$).

FIG. 6. EFFECT OF GROUND BOUNDARY LAYER ON C_L (NO TAILPLANE) v α_w.
GROUND CLEARANCE 1·5$\bar{c}$, WITH FUSELAGE B.L.C. FOR FULL α_w RANGE (0^0-20^0).

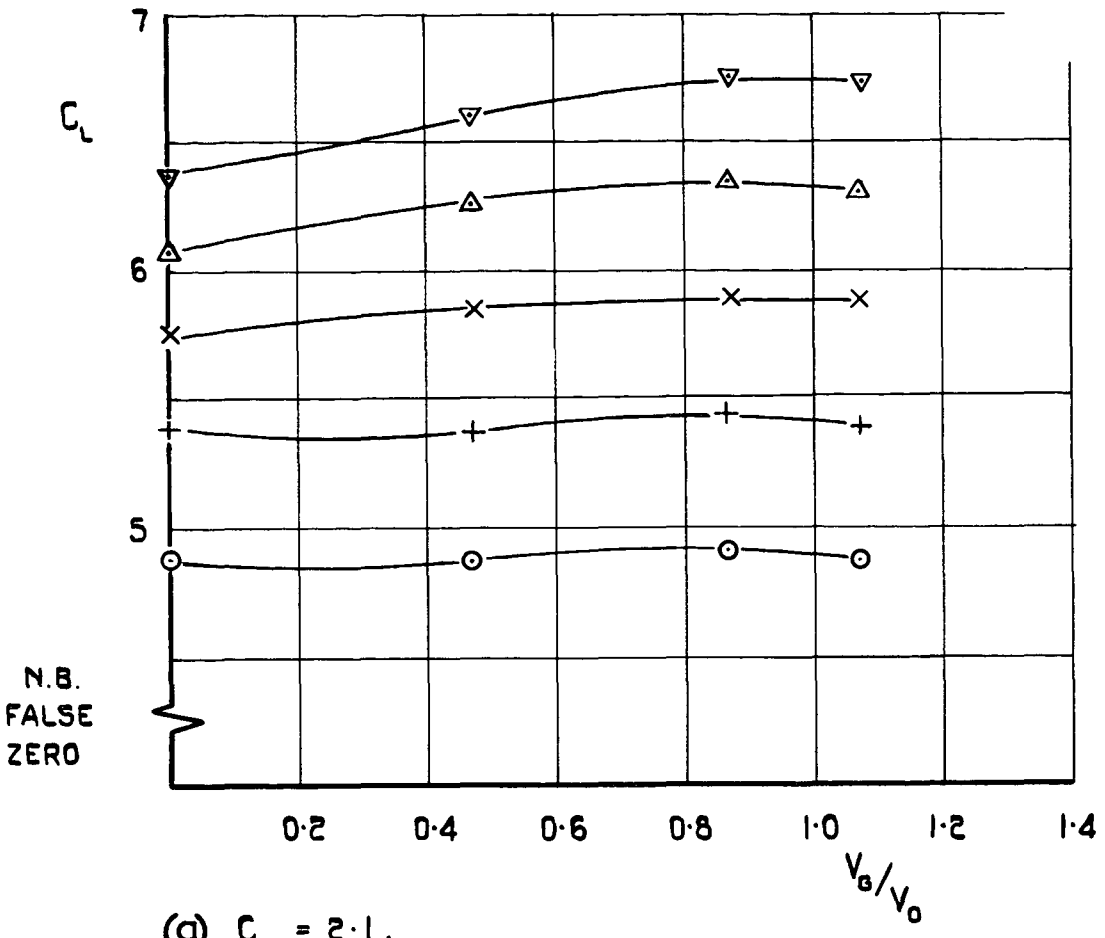

(a) $C_\mu = 2{\cdot}1$.

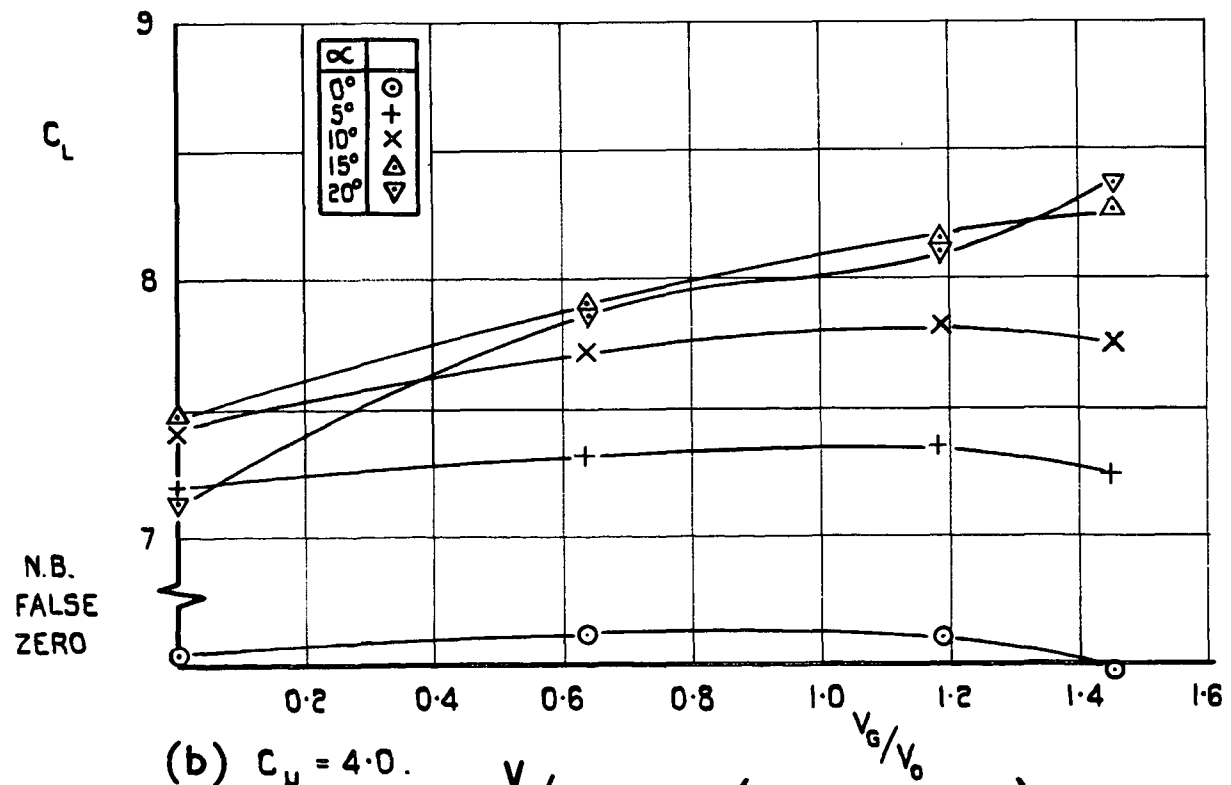

(b) $C_\mu = 4{\cdot}0$.

FIG. 7. EFFECT OF V_G/V_0 ON C_L (NO TAILPLANE)
AT CONSTANT INCIDENCE. CONTROL ANGLE 30° ($\theta \doteq 50°$), GROUND CLEARANCE 1·5 $\bar{\bar{c}}$.

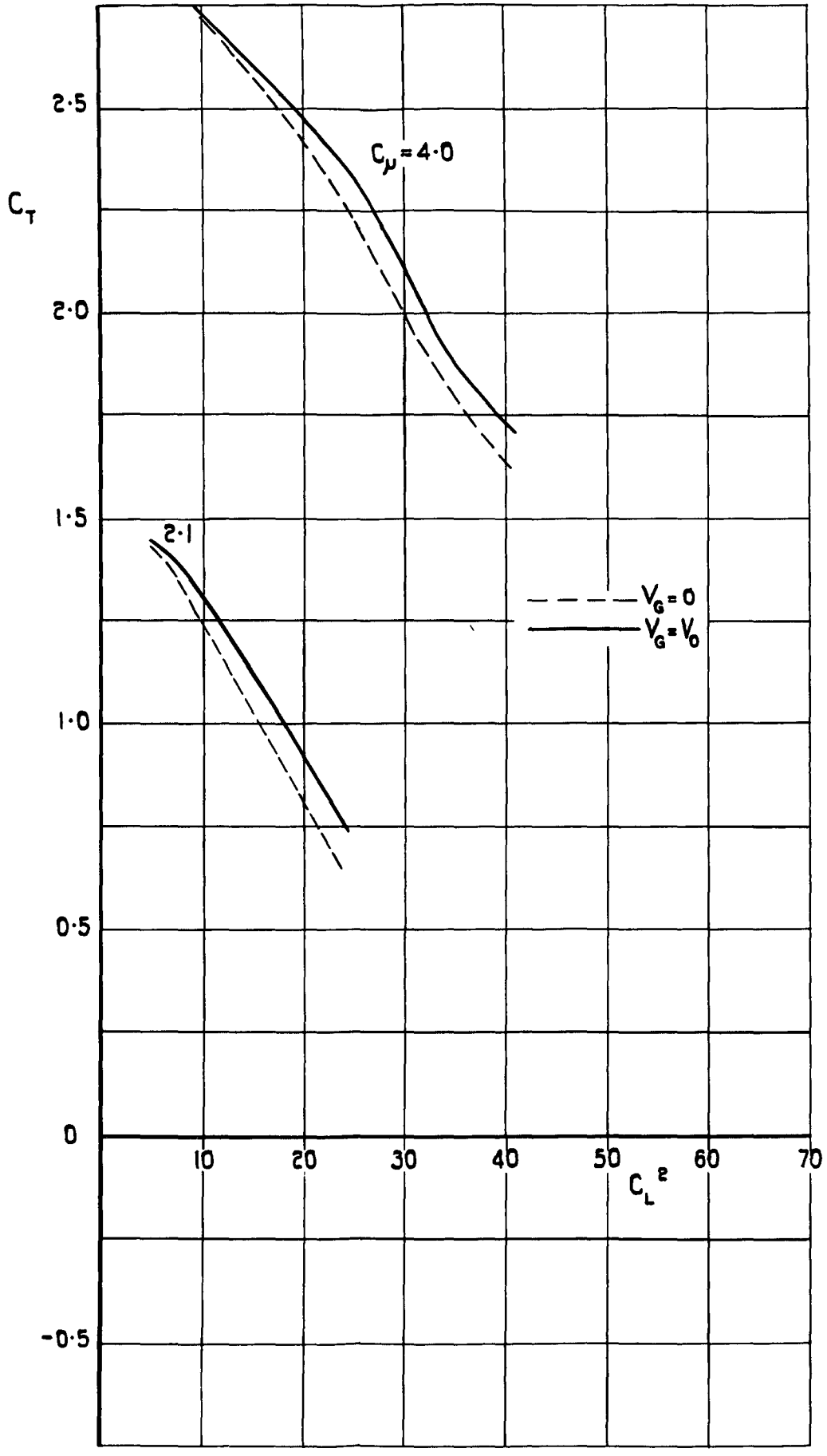

(a) CONTROL ANGLE = 0° ($\theta \triangleq 20°$).

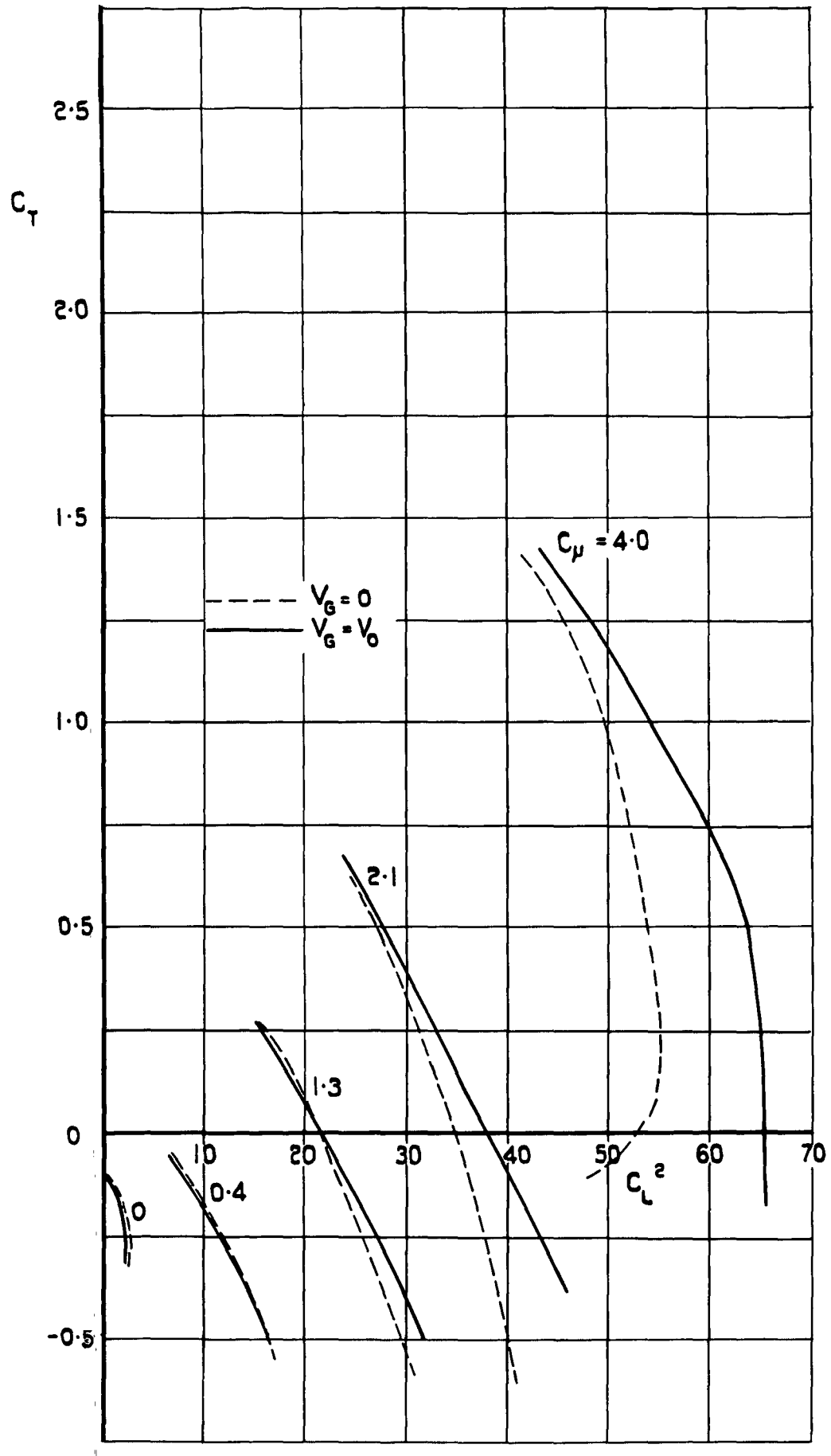

(b) CONTROL ANGLE = 30° ($\theta \triangleq 50°$).

FIG. 8. EFFECT OF GROUND BOUNDARY LAYER ON C_T v C_L^2 (NO TAILPLANE). GROUND CLEARANCE $1.5\bar{\bar{c}}$.

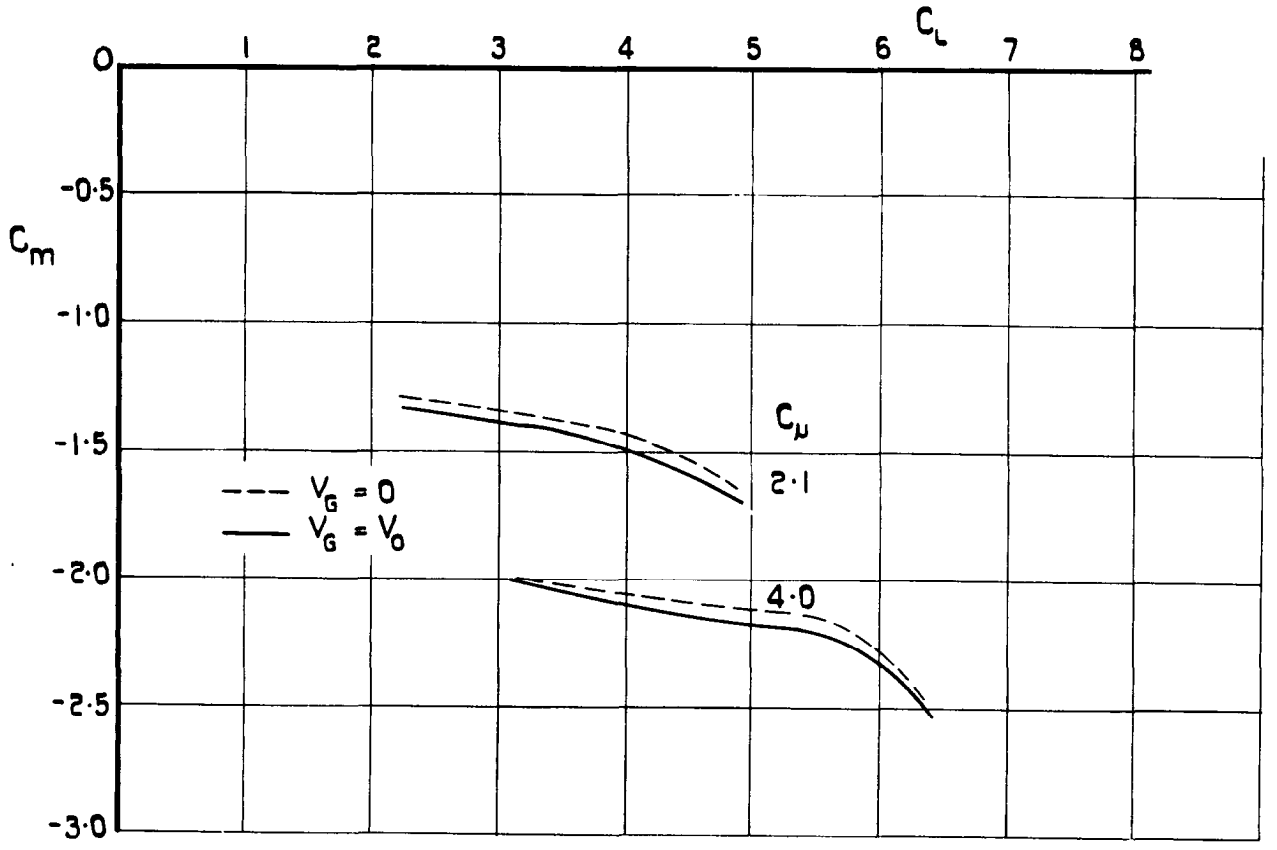

(a) CONTROL ANGLE = 0° ($\theta \triangleq 20°$).

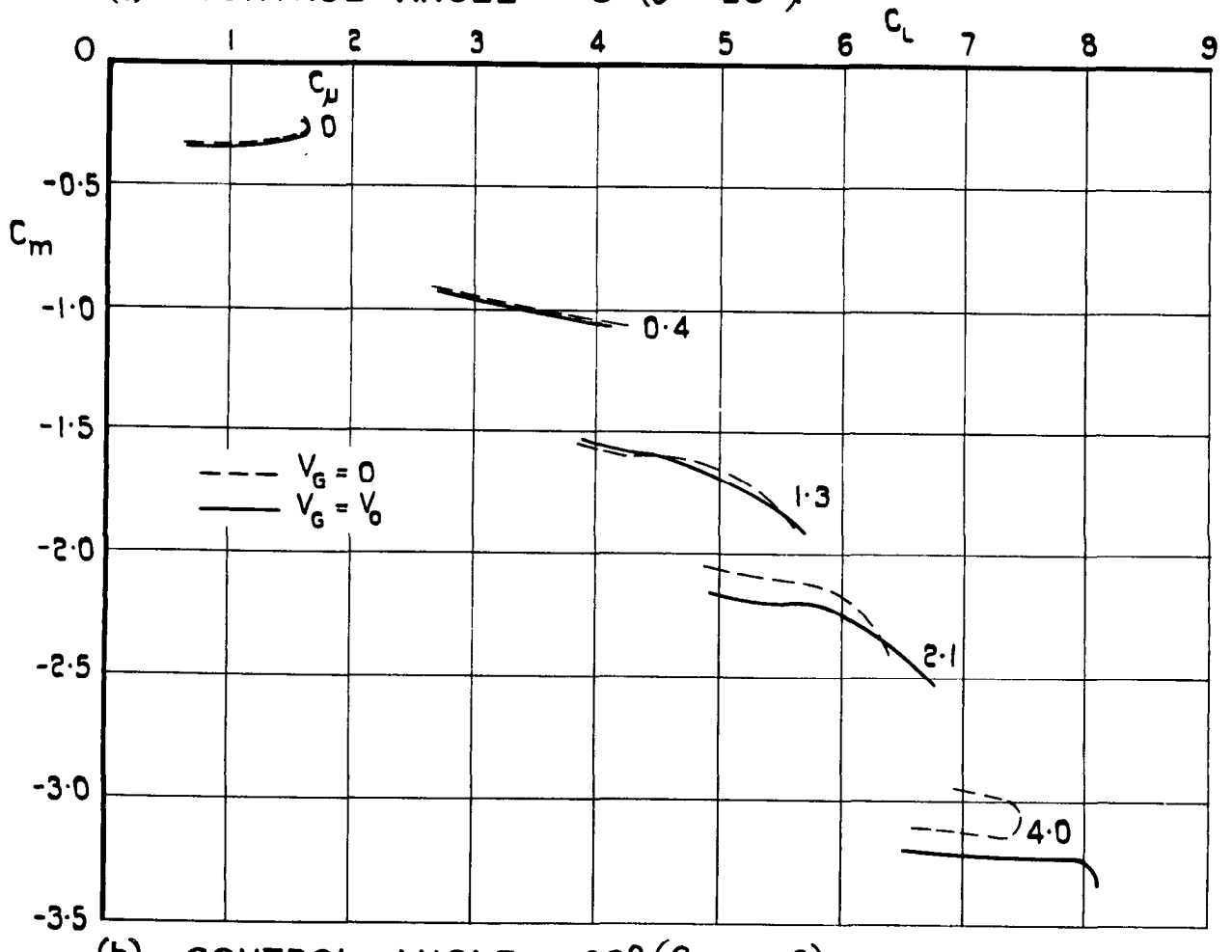

(b) CONTROL ANGLE = 30° ($\theta \triangleq 50°$).

FIG. 9. EFFECT OF GROUND BOUNDARY LAYER ON C_m V C_L (NO TAILPLANE). GROUND CLEARANCE 1·5$\bar{\bar{c}}$.

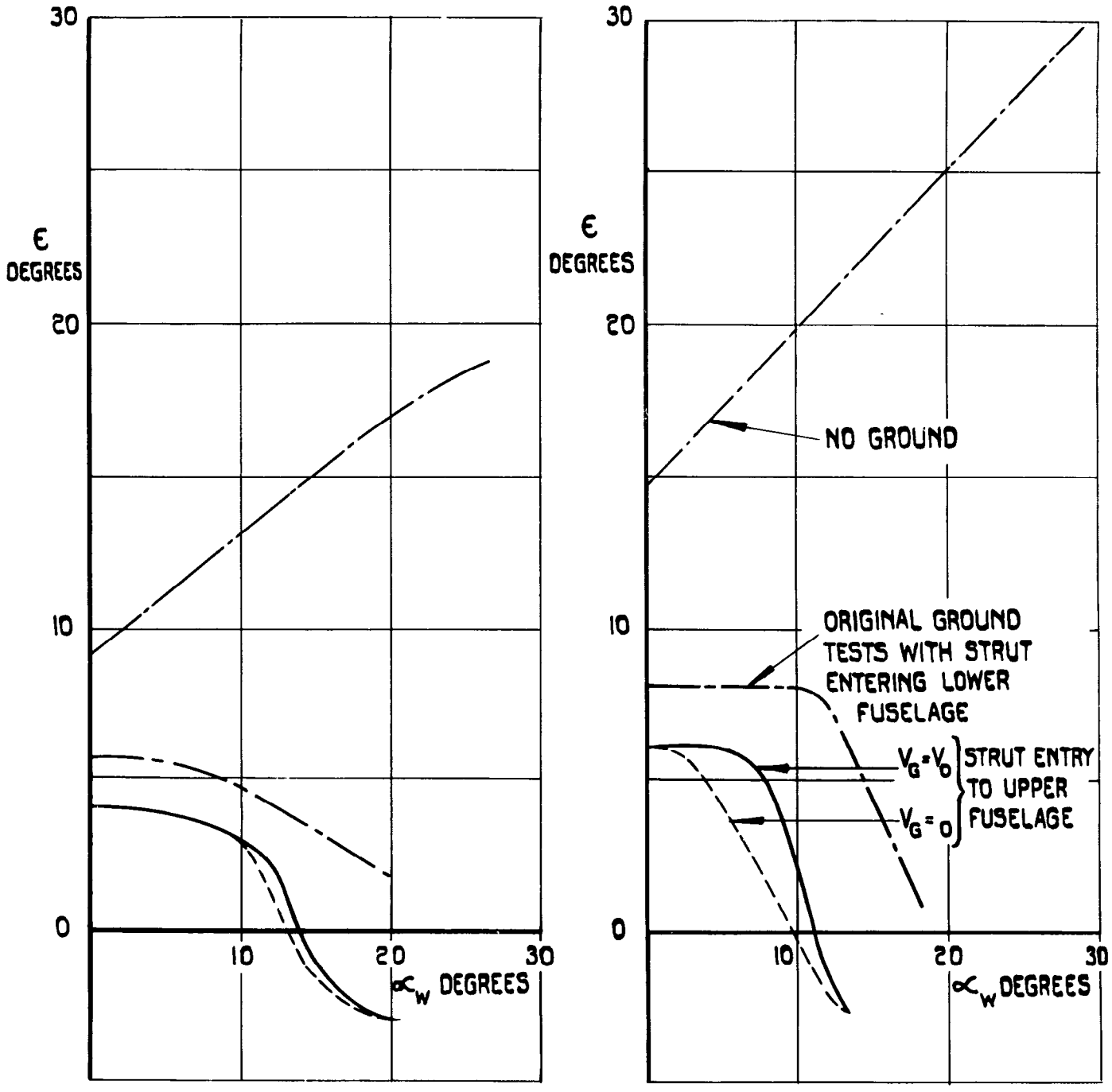

(a) $C_\mu = 0{\cdot}4$.

(b) $C_\mu = 2{\cdot}1$.

FIG.10. EFFECT OF GROUND BOUNDARY LAYER ON ϵ v α_w.
CONTROL ANGLE = 30° ($\theta \simeq 50°$), GROUND CLEARANCE 1·5$\bar{\bar{c}}$.

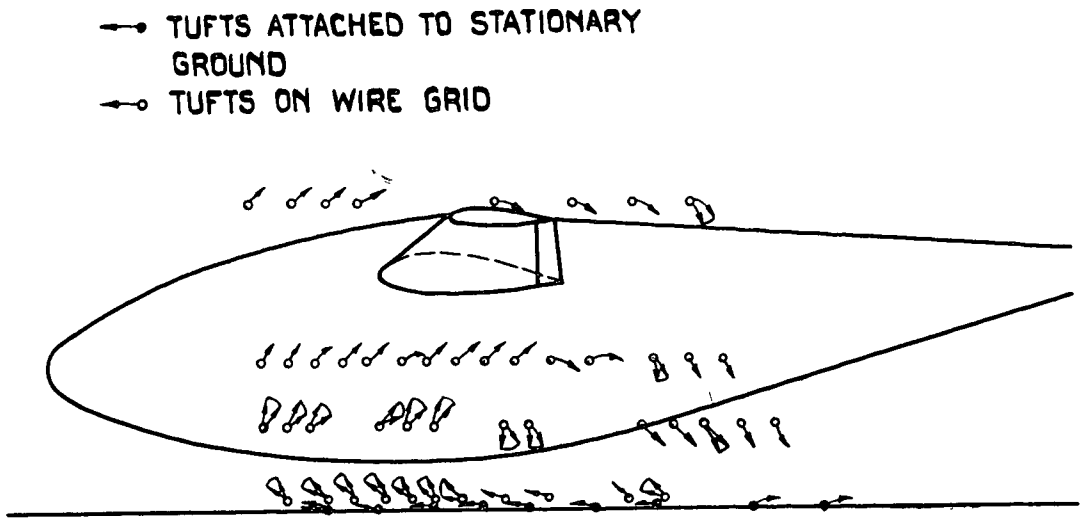

(i) $\alpha_w = 5°$.

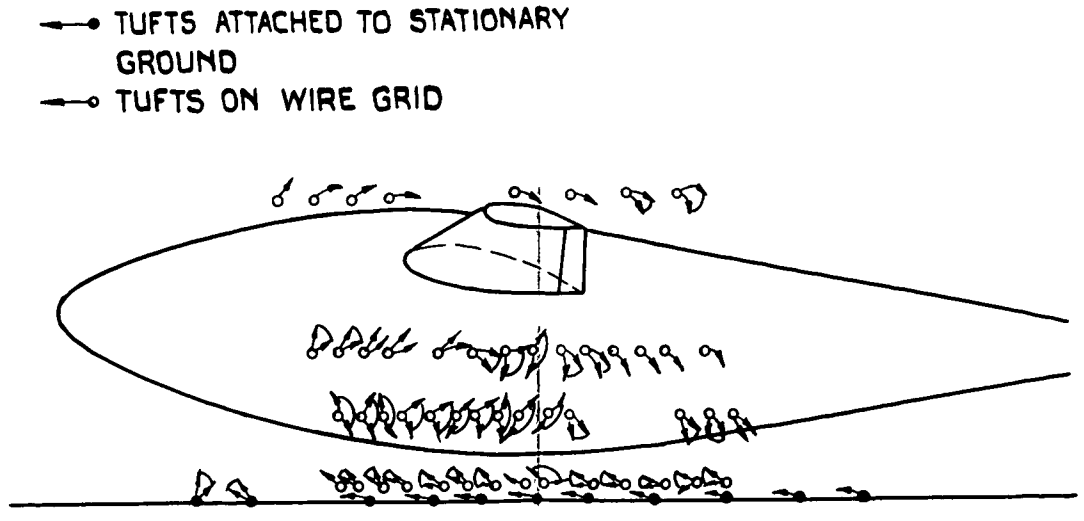

(i) $\alpha_w = 15°$.

(a) GROUND BELT STATIONARY.

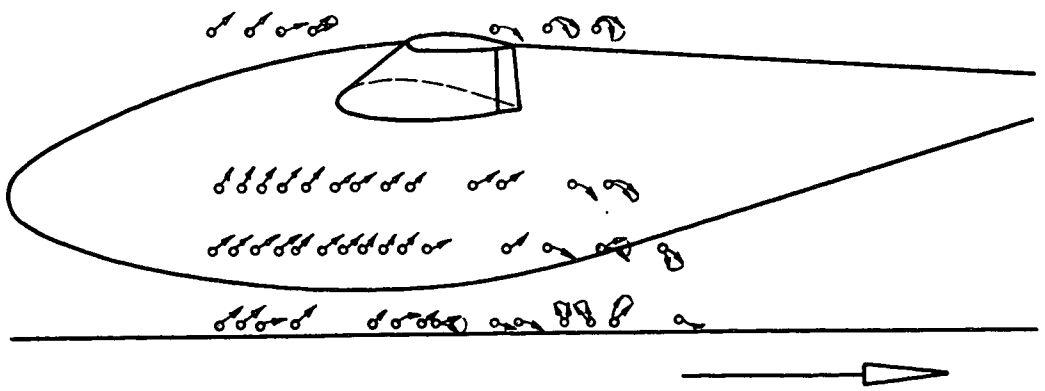

(i) $\alpha_w = 5°$.

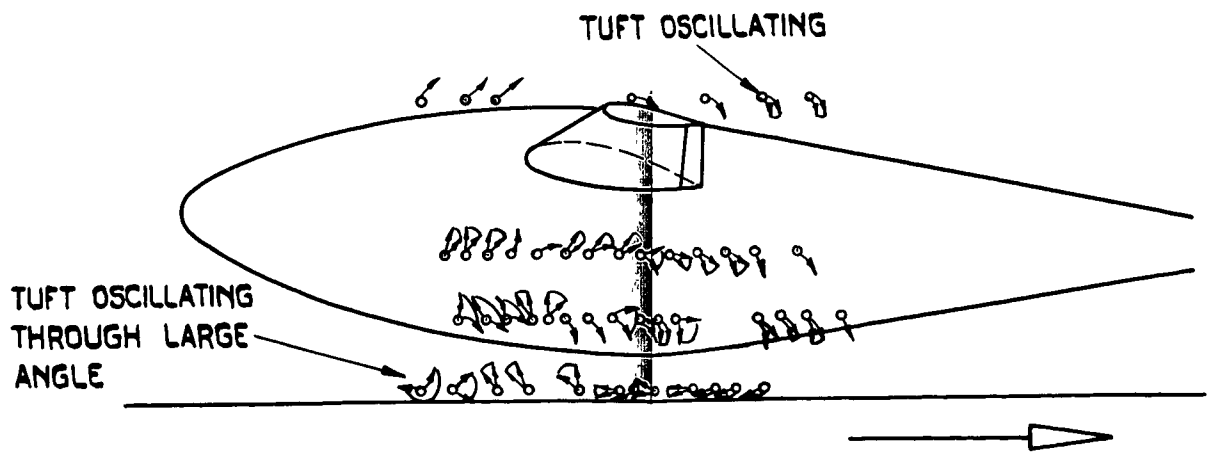

(i) $\alpha_w = 15°$.

(b) GROUND BELT MOVING, $V_G = V_0$.

FIG. 11. FLOW FIELD WITH JET IMPINGEMENT ON THE GROUND. CONTROL ANGLE 30° ($\theta \simeq 50°$), $C_\mu = 4.0$, GROUND CLEARANCE 1.5 c.

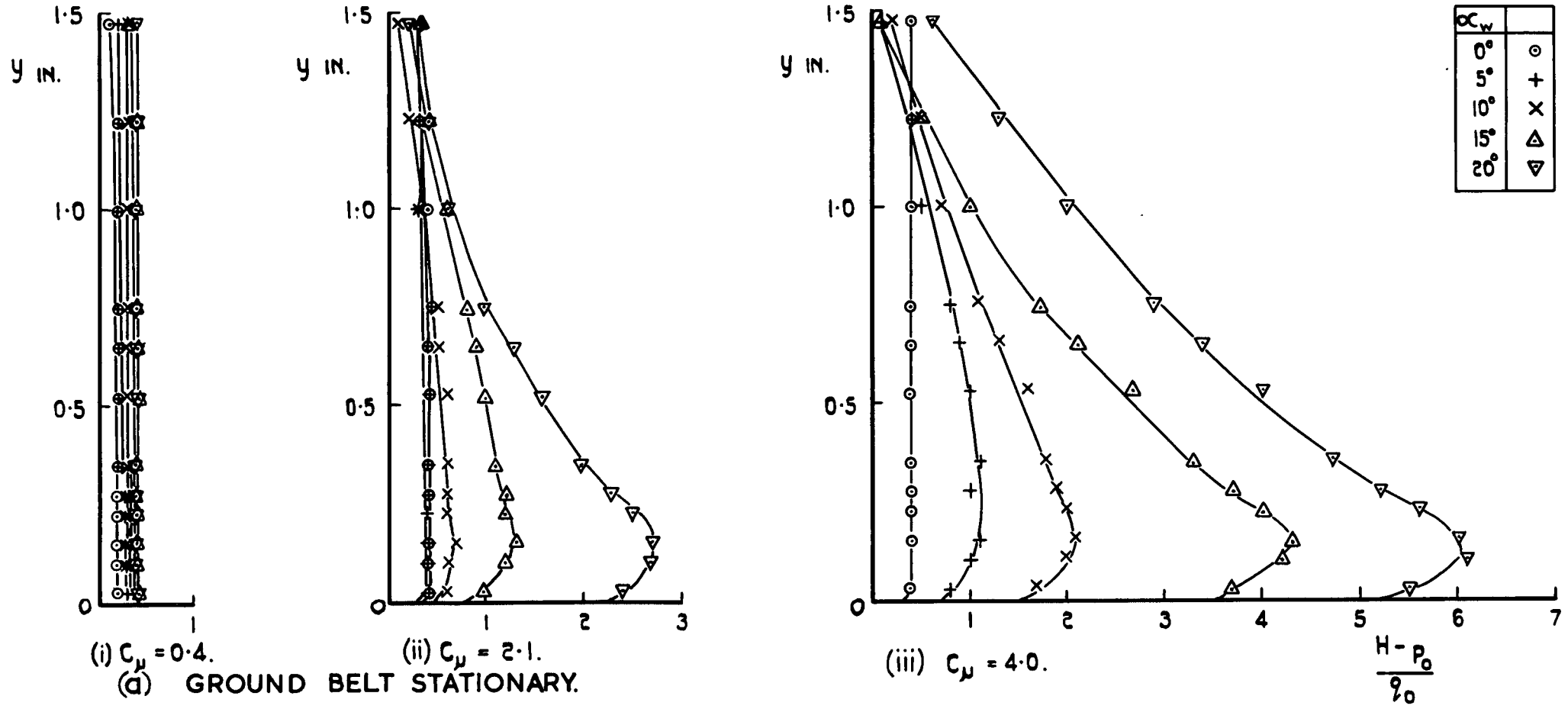

FIG.12. GROUND BOUNDARY-LAYER PROFILES 0·6 LOCAL CHORDS BEHIND THE WING L.E. PLANE. REARWARD-FACING RAKE. CONTROL ANGLE = 30° ($\theta \triangleq 50°$), GROUND CLEARANCE 1·5$\bar{\bar{c}}$, TRAVERSE IN PLANE OF WING MID-SEMI-SPAN.

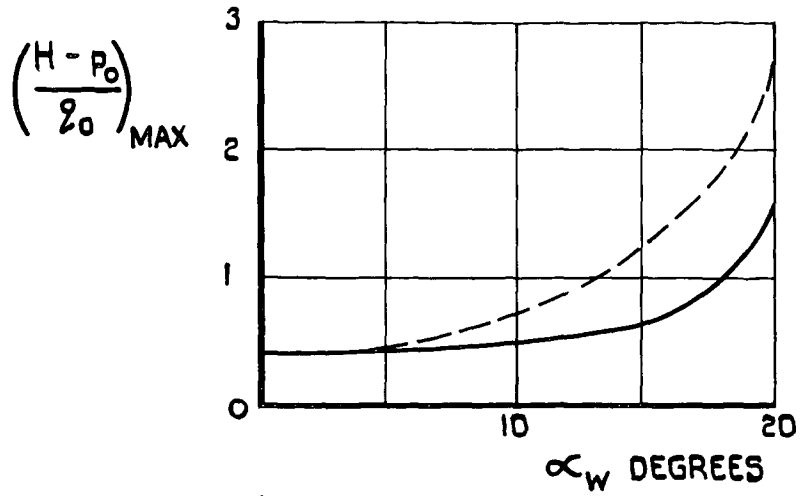

(a) $C_\mu = 2{\cdot}1.$

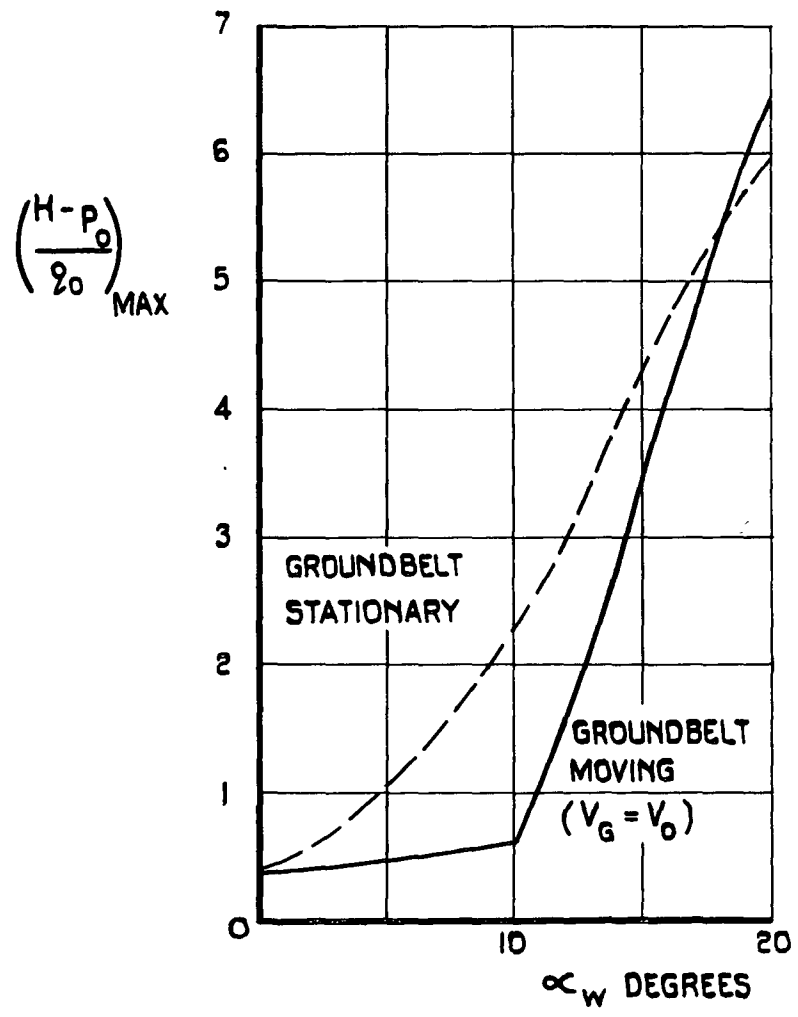

(b) $C_\mu = 4{\cdot}0.$

FIG.13. EFFECT OF GROUND SURFACE MOVEMENT ON $\left(\frac{H-p_0}{\rho_0}\right)_{MAX.}$ IN GROUND BOUNDARY LAYER AT 0·6 LOCAL CHORDS BEHIND WING L.E. PLANE. REARWARD-FACING RAKE. CONTROL ANGLE 30° ($\theta \triangleq 50°$), GROUND CLEARANCE $1{\cdot}5\bar{c}$, TRAVERSE OF GROUND BOUNDARY LAYER IN PLANE OF WING MID-SEMI-SPAN.

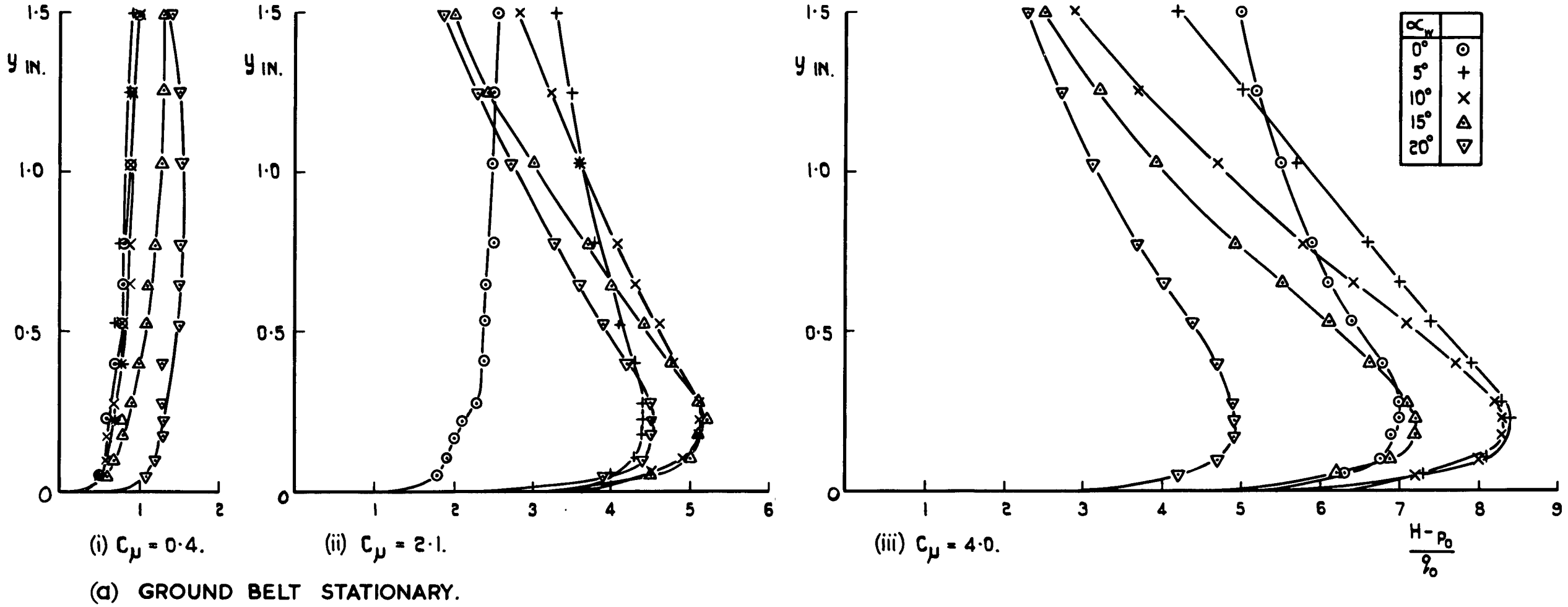

(a) GROUND BELT STATIONARY.

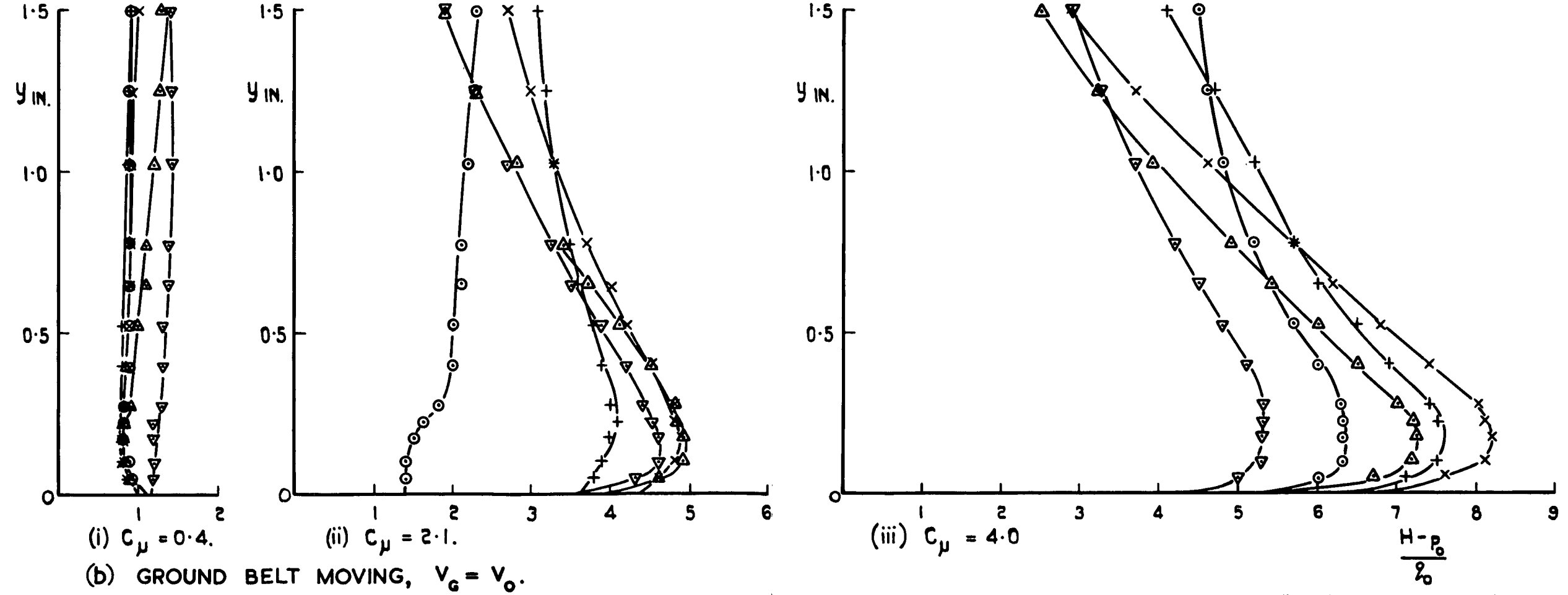

(b) GROUND BELT MOVING, $V_G = V_0$.

FIG.14. GROUND BOUNDARY-LAYER PROFILES 3·2 LOCAL CHORDS BEHIND THE WING L.E. PLANE. FORWARD-FACING RAKE. CONTROL ANGLE = 30° ($\theta \triangleq 50°$), GROUND CLEARANCE .5 $\bar{c}$, TRAVERSE IN PLANE OF WING MID-SEMI-SPAN.

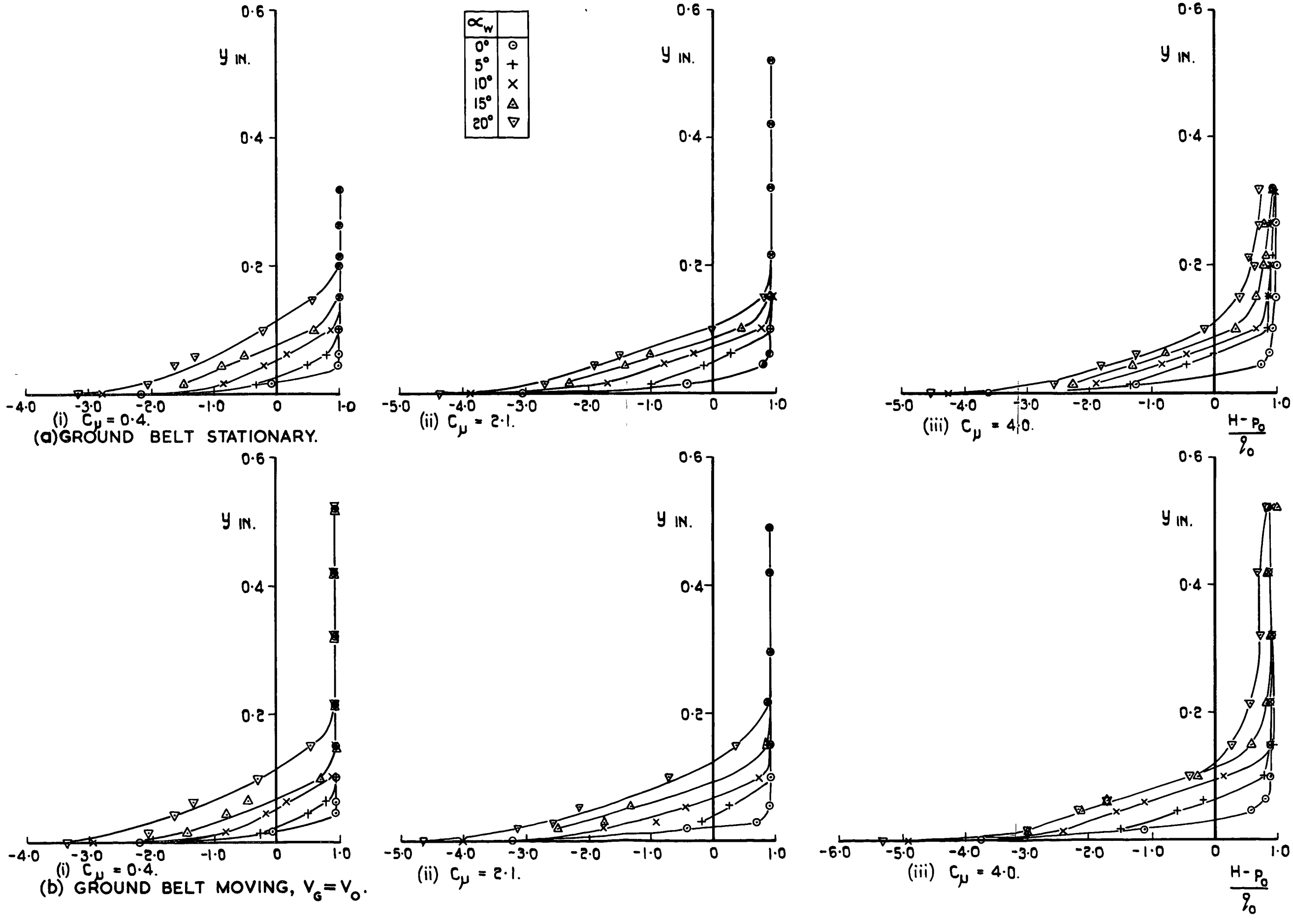

FIG. 15. WING UPPER SURFACE BOUNDARY-LAYER PROFILES AT WING MID-SEMI-SPAN.
CONTROL ANGLE 30° ($\theta \simeq 50°$), GROUND CLEARANCE 1·5 $\bar{c}$, FORWARD-FACING RAKE AT 40% CHORD.

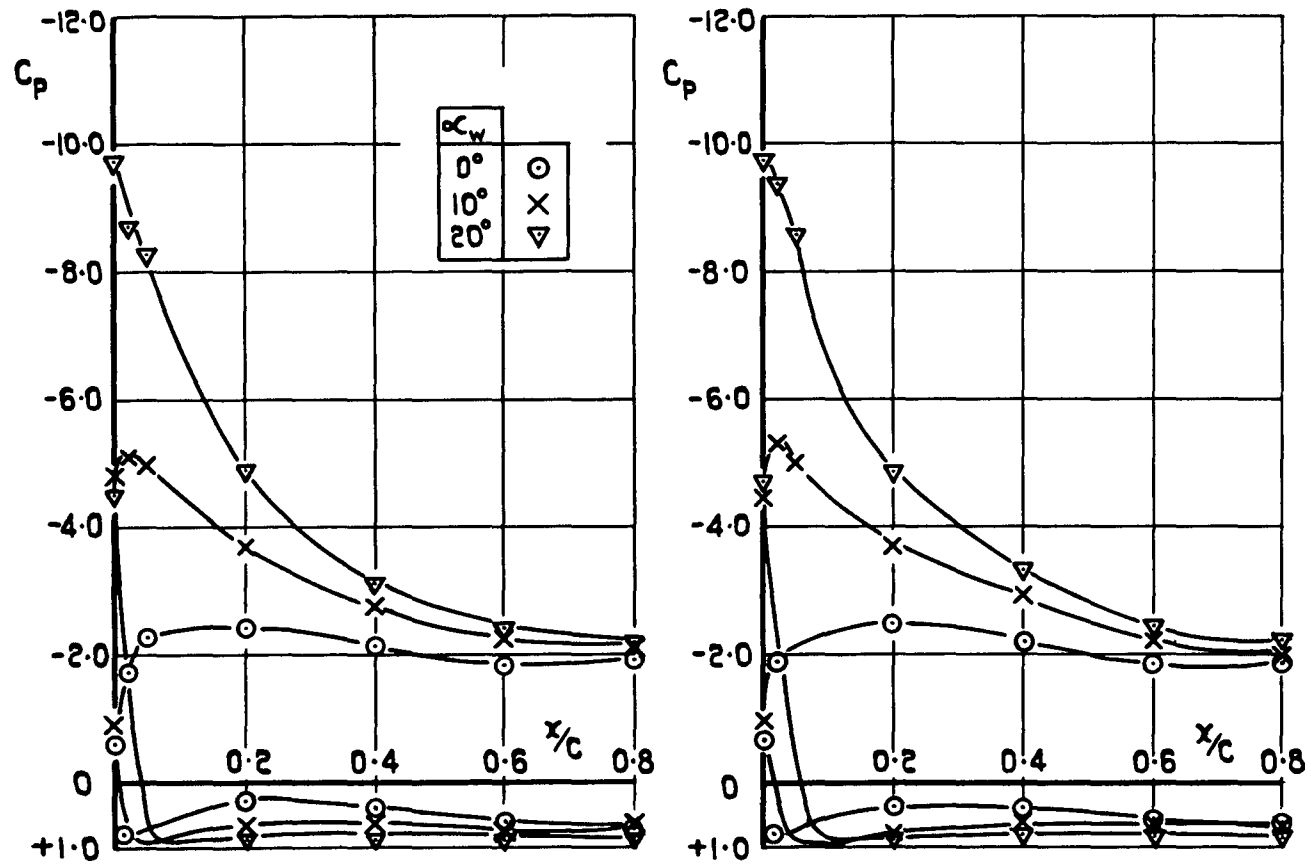

(a) GROUND BELT STATIONARY. (b) GROUND BELT MOVING, $V_G = V_o$.

FIG. 16. CHORDWISE C_p DISTRIBUTIONS AT WING MID-SEMI-SPAN WITH $\theta \doteq 50°$, $C_\mu = 0·4$, GROUND CLEARANCE $1·5\,\bar{c}$.

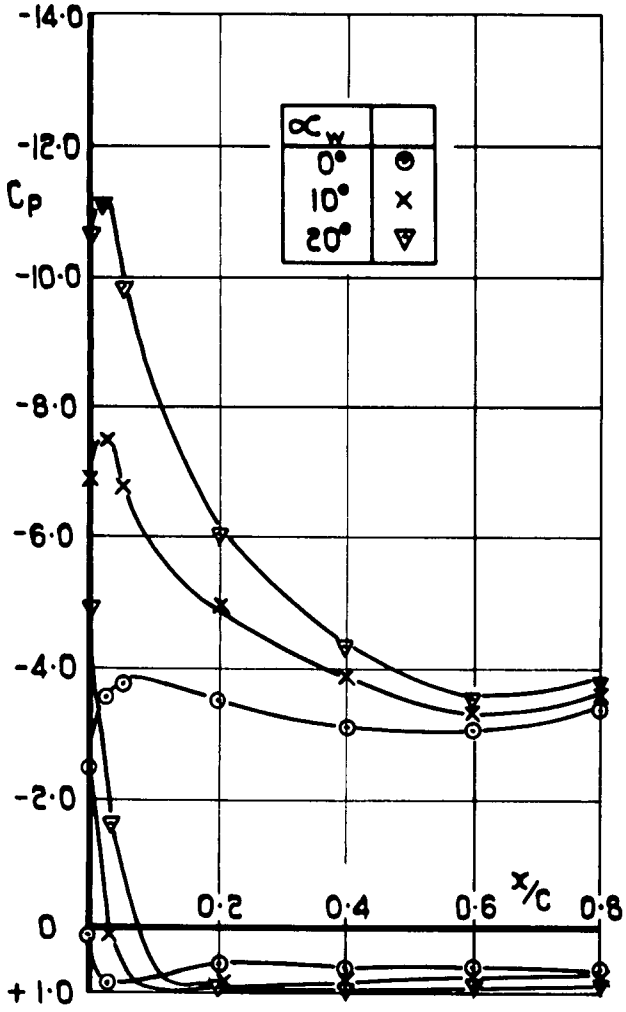

(a) GROUND BELT STATIONARY.

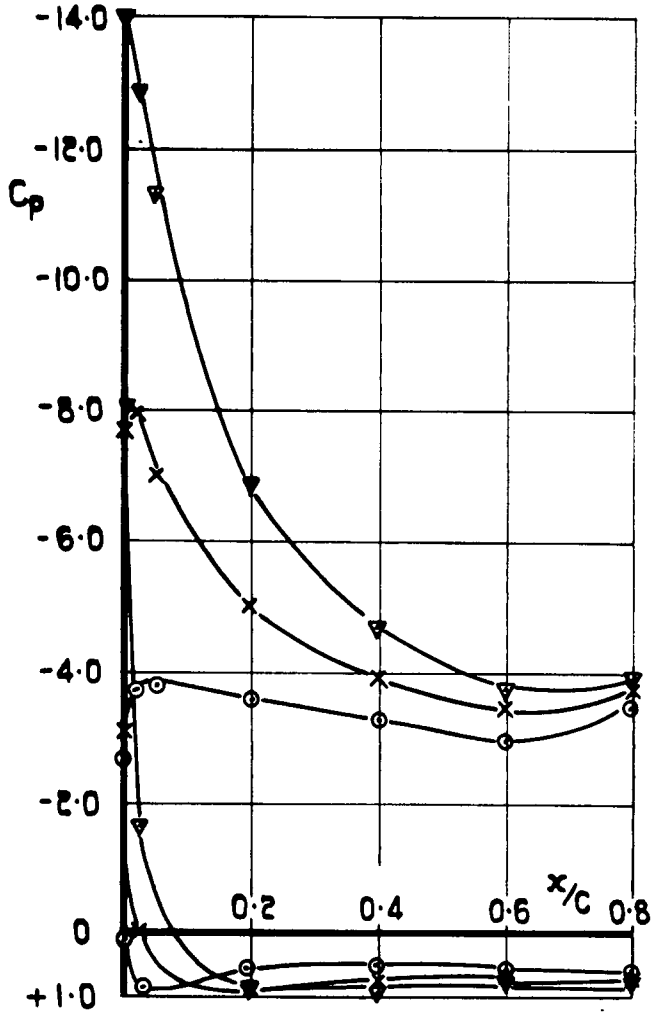

(b) GROUND BELT MOVING, $V_G = V_O$.

FIG. 17. CHORDWISE C_p DISTRIBUTIONS AT WING MID-SEMI-SPAN WITH $\theta \triangleq 50°$, $C_\mu = 2{\cdot}1$, GROUND CLEARANCE $1{\cdot}5\bar{\bar{c}}$.

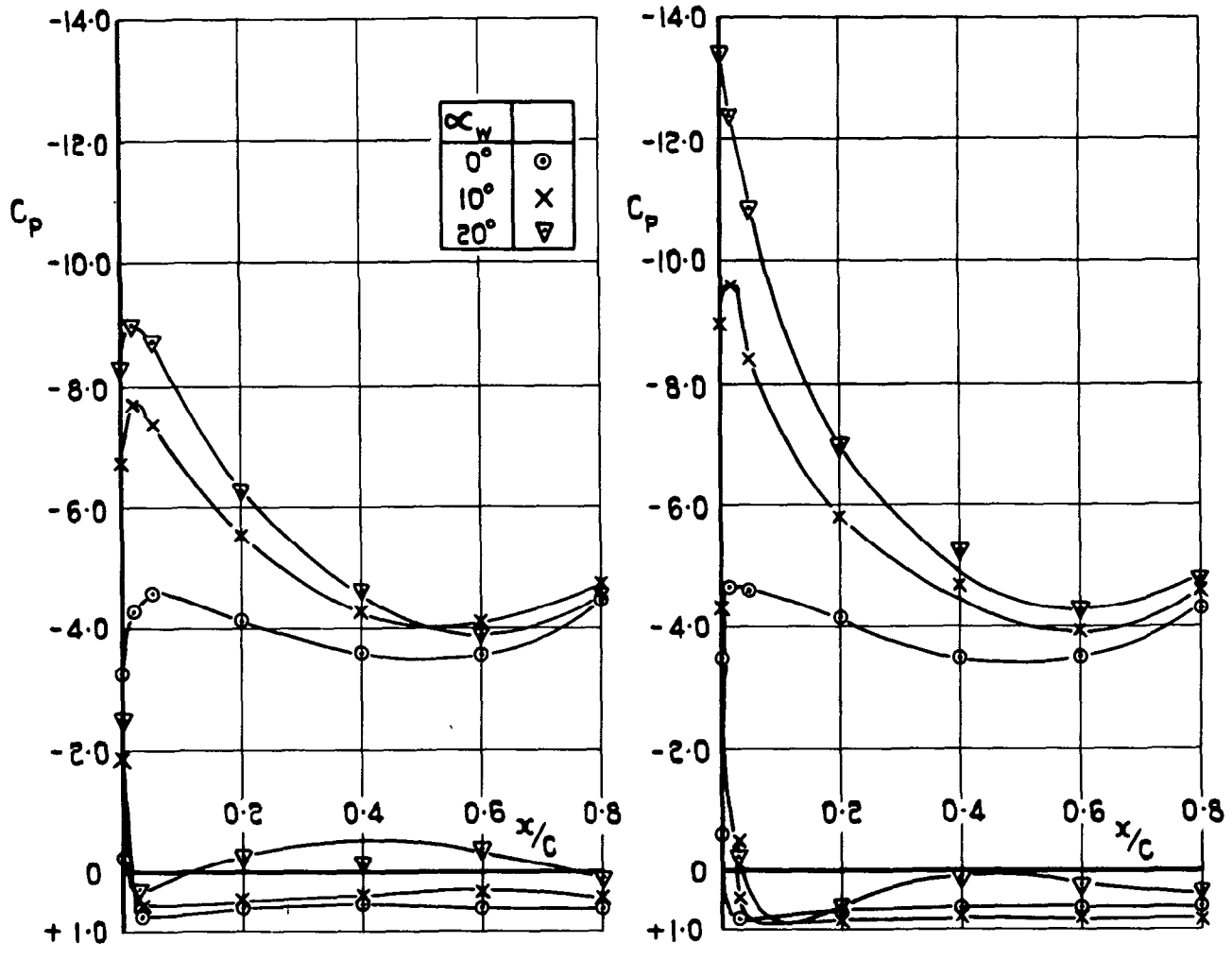

(a) GROUND BELT STATIONARY. (b) GROUND BELT MOVING, $V_G = V_O$.

FIG.18. CHORDWISE C_p DISTRIBUTIONS AT WING MID-SEMI-SPAN WITH $\theta \simeq 50°$, $C_\mu = 4 \cdot 0$, GROUND CLEARANCE $1 \cdot 5 \bar{c}$.

Printed in England for Her Majesty's Stationery Office by the Royal Aircraft Establishment, Farnborough. Dd.125875. K.4.

A.R.C. C.P. No.849 533.6.071.1 : 533.682 : 5.001.58 :

LOW-SPEED TUNNEL TESTS OF AN A.R.9 JET-FLAP MODEL, WITH GROUND SIMULATION BY MOVING-BELT RIG. 533.652.6 : 533.694.6

Butler, S.F.J., Moy, B.A. and Hutchins, G.D. April 1964.

In order to assess the adequacy of the conventional stationary tunnel groundboard technique, particularly for V/STOL models exhibiting large, and often adverse, ground effects, tests have been made on some representative models, including the experiments on a jet-flap model discussed in the present Note. By use of the moving-belt rig, the spurious relative motion between the mainstream and the simulated ground surface could be eliminated and more representative ground boundary-layer flows could be achieved.

(Over)

A.R.C. C.P. No.849 533.6.071.1 : 533.682 : 5.001.58 :

LOW-SPEED TUNNEL TESTS OF AN A.R.9 JET-FLAP MODEL, WITH GROUND SIMULATION BY MOVING-BELT RIG. 533.652.6 : 533.694.6

Butler, S.F.J., Moy, B.A. and Hutchins, G.D. April 1964.

In order to assess the adequacy of the conventional stationary tunnel groundboard technique, particularly for V/STOL models exhibiting large, and often adverse, ground effects, tests have been made on some representative models, including the experiments on a jet-flap model discussed in the present Note. By use of the moving-belt rig, the spurious relative motion between the mainstream and the simulated ground surface could be eliminated and more representative ground boundary-layer flows could be achieved.

(Over)

A.R.C. C.P. No.849 533.6.071.1 : 533.682 : 5.001.58 :

LOW-SPEED TUNNEL TESTS OF AN A.R.9 JET-FLAP MODEL, WITH GROUND SIMULATION BY MOVING-BELT RIG. 533.652.6 : 533.694.6

Butler, S.F.J., May, B.A. and Hutchins, G.D. April 1964.

In order to assess the adequacy of the conventional stationary tunnel groundboard technique, particularly for V/STOL models exhibiting large, and often adverse, ground effects, tests have been made on some representative models, including the experiments on a jet-flap model discussed in the present Note. By use of the moving-belt rig, the spurious relative motion between the mainstream and the simulated ground surface could be eliminated and more representative ground boundary-layer flows could be achieved.

(Over)

With the jet-flap model, the ground boundary-layer condition only had an important influence once jet sheet impingement occurred. Thus, the wing incidence at which an appreciable proportion of the jet efflux flowed upstream along the ground was some 10^{0} higher with the ground surface in motion. The use of a moving ground surface was preferable under these conditions, since it resulted in appreciably higher values of wing lift and stalling incidence, as well as changes in drag, pitching moments, and downwash.

Apart from such favourable modifications at very high lift ($C_L \geq 7$), these tests generally confirmed the original fixed groundboard tests, which have been used to predict the take-off and landing behaviour of the B.A.C. 126 jet-flap research aircraft.

With the jet-flap model, the ground boundary-layer condition only had an important influence once jet sheet impingement occurred. Thus, the wing incidence at which an appreciable proportion of the jet efflux flowed upstream along the ground was some 10^{0} higher with the ground surface in motion. The use of a moving ground surface was preferable under these conditions, since it resulted in appreciably higher values of wing lift and stalling incidence, as well as changes in drag, pitching moments, and downwash.

Apart from such favourable modifications at very high lift ($C_L \geq 7$), these tests generally confirmed the original fixed groundboard tests, which have been used to predict the take-off and landing behaviour of the B.A.C. 126 jet-flap research aircraft.

With the jet-flap model, the ground boundary-layer condition only had an important influence once jet sheet impingement occurred. Thus, the wing incidence at which an appreciable proportion of the jet efflux flowed upstream along the ground was some 10^{0} higher with the ground surface in motion. The use of a moving ground surface was preferable under these conditions, since it resulted in appreciably higher values of wing lift and stalling incidence, as well as changes in drag, pitching moments, and downwash.

Apart from such favourable modifications at very high lift ($C_L \geq 7$), these tests generally confirmed the original fixed groundboard tests, which have been used to predict the take-off and landing behaviour of the B.A.C. 126 jet-flap research aircraft.

C.P. No. 849

Published by
HER MAJESTY'S STATIONERY OFFICE
To be purchased from
49 High Holborn, London W.C.1
423 Oxford Street, London W.1
13A Castle Street, Edinburgh 2
109 St. Mary Street, Cardiff
Brazennose Street, Manchester 2
50 Fairfax Street, Bristol 1
35 Smallbrook, Ringway, Birmingham 5
80 Chichester Street, Belfast 1
or through any bookseller

C.P. No. 849

S.O. CODE No. 23-9016-49